Manufacturing Rev. **10**, 10 (2023)

https://doi.org/10.1051/mfreview/2023009

Manufacturing Review
Available online at:
https://mfr.edp-open.org

REVIEW

OPEN ACCESS

A review on conventional and nonconventional machining of Nickel-based Nimonic superalloy

Ganesha Prasad, Raghavendra Kamath C.**, and Vijay G.S.*

Department of Mechanical and Industrial Engineering, Manipal Institute of Technology, Manipal Academy of Higher Education, Manipal 576104, Karnataka, India

Received: 19 September 2022 / Accepted: 21 April 2023

Abstract. Superalloys have gained prominence in recent years in various sectors, namely, spacecraft, marine, power, defense, vehicular and others, due to their ability to withstand high temperatures of up to 980 °C without deformation. Nimonics are Nickel-based superalloys usually known to be hard-to-machine materials due to their high strength at high temperatures, higher hardness, low thermal conductivity, and tendency to react with tool material. All these factors increase the level of difficulties in the machining of Nimonic superalloys. Numerous studies have examined various facets of machining of Nimonic alloys. This article summarizes the observation from 152 research articles to offer a reasonable engineering overview of the study of Nimonic alloys. An overview of Nimonic superalloys and their applications is given first. Then, various conventional and non-conventional machining processes, problems associated with multiple machining processes and methods to rectify the issues concerning the machining process have been reported. Thus, this summary will certainly help industrialists and academic researchers for further research work in machining Nimonic alloys.

Keywords: Nimonic / Nickel-based superalloys / turning / milling / EDM / WEDM

1 Introduction

The term 'superalloy' came into existence shortly after the second world war and is used to describe a group of materials capable of sustaining their properties even at higher temperatures [1]. Superalloys are uncommon materials because of their excellent physical and chemical properties, such as superior mechanical and thermal strength, good fatigue resistance, better surface stability, and resistance to oxidation or corrosion [2]. Superalloys have gained prominence in recent years in various sectors, namely, spacecraft, marine, power, defense, vehicular and others, due to their ability to withstand high temperatures of up to 980 °C without deformation. The crystal structure of the superalloys is usually a face-centered cubic austenitic phase. The superalloys are generally employed in high-temperature environments (above 650 °C) like in gas turbines (Figure 1), aero engines (Figure 2), nuclear power plants, chemical and petrochemical plants, paper and pulp industry, food processing plants, and rocket engines. The commonly used superalloys include Inconel [3], Haynes [4], Monel [5], Nimonic, Incoloy [6], Waspaloy [7], Hastelloy [2], and many more. A superalloy is a combination of metals like Ni, Co, Cr, and Fe from the VIIIB group in the periodic table and some other metals like Al, Ta, Mo, Nb, W, and Ti in lesser proportion [8]. There are three categories of superalloys classified based on more significant percentages of certain metal content, namely, Ni-based, Co-based, and Fe-based. Amongst all the superalloys, Ni-based superalloys have a much better capability to retain the properties at high temperatures near the melting point and have good resistance to oxidation and creep due to the presence of Ni-Al-Ti in the precipitation form in the Ni-Cr matrix. The various alloying elements in the Ni-based superalloy and their role is given in Table 1 [9,10].

The presence of Ni in the higher proportions has caused Ni-based superalloys to be expensive and hard to machine. The Ni-based superalloys belong to the orange group (group S) in the ISO classification of materials, wherein they are strengthened by the precipitation of gamma prime (FCC structure) consisting of Al and Ti in the interchangeable form [1,4]. Hence, a higher cutting force is required to machine the Ni-based superalloys due to their increased hardness, making them difficult to machine. While machining Ni-based superalloys under dry conditions at higher cutting speed (CS) and depth of cut (DOC), surface cavities are formed. On the other hand, while dry machining at a lower CS, rapid tool wear is

*Corresponding author: vijay.gs@manipal.edu
**Corresponding author: cr.kamath@manipal.edu

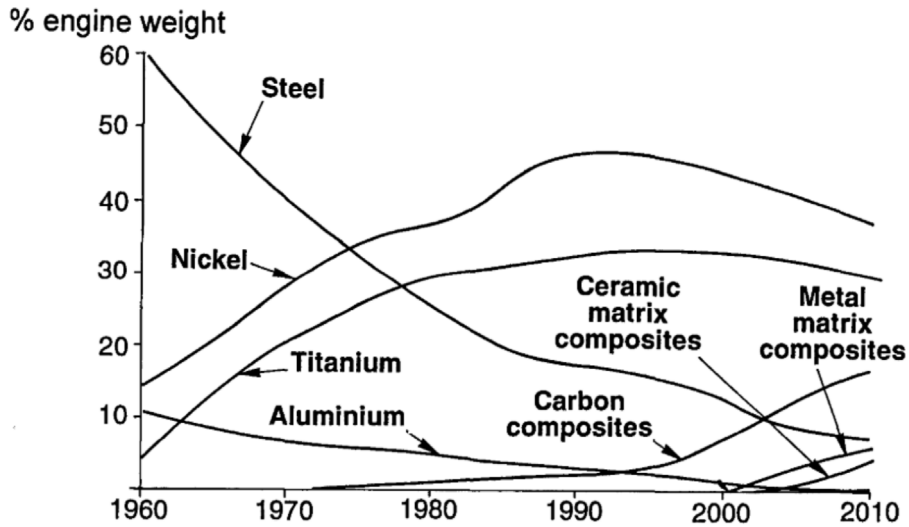

Fig. 1. Use of materials in aero gas turbines [13]; a rise on the use of Ni and Ti in gas turbines is evident.

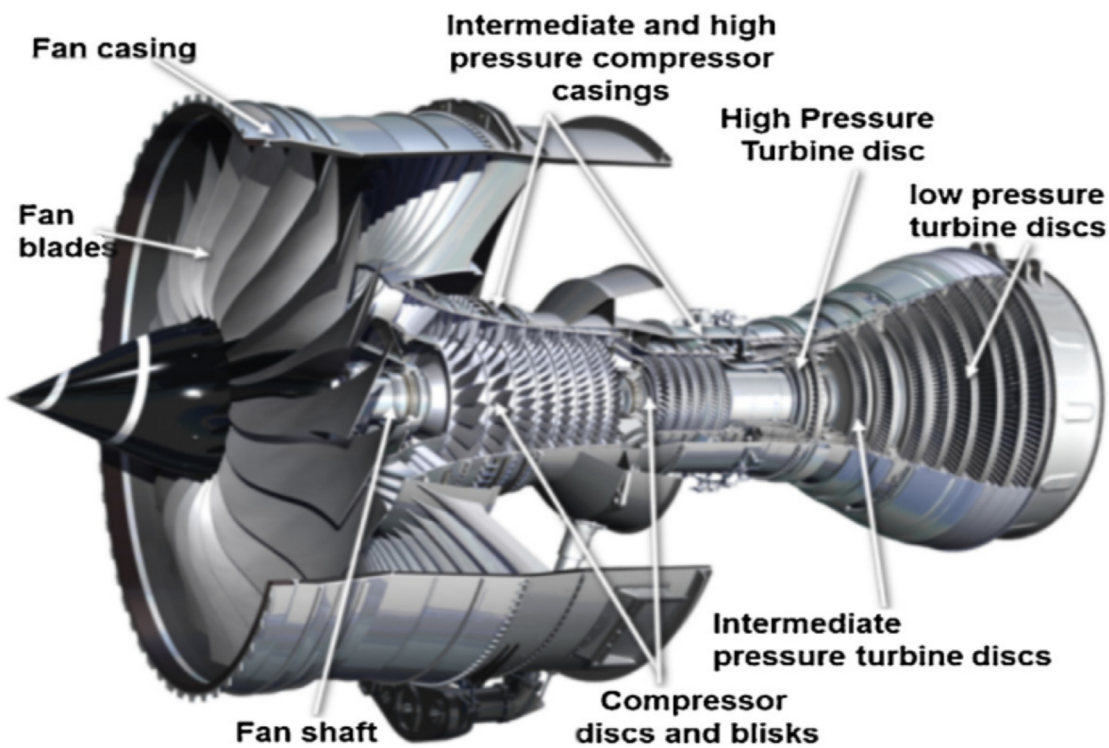

Fig. 2. Application of superalloys in Rolls-Royce XWB turbofan engine [14].

observed along with longer machining time and higher machining cost. Since the machining of Ni-based superalloys generates higher temperatures and higher cutting force, the tool cutting edge is subjected to a higher load. In addition, once the specific cutting energy exceeds 3000 Nmm/mm^3, chipping of the cutting edge is observed [4]. All the above factors make the Ni-based superalloy a hard-to-machine material.

Nimonic superalloys are Al-rich Ni alloys, having a cubic $L1_2$ structure and chemical phase Ni_3 (Al, Ti) [15]. The properties of these alloys include better thermal stability, corrosion resistance, and retention of mechanical properties (wear resistance, hardness, yield strength, impact strength, and facture toughness). Researchers have worked on different Nimonic superalloys viz., Nimonic 75, Nimonic 80A, Nimonic 90, and Nimonic C263, to name a few, and have reported valuable findings. Nimonic 75 was introduced in the 1940s, and was used in the turbine blades of the Whittle jet engine. It is a 80/20 Ni-Cr alloy with limited addition of Ti and C. Nowadays, Nimonic 75 is commonly used in sheet metal applications due to its good

Table 1. Role of alloying elements in Ni-based superalloy [11,12].

Element	Effects
Nickel (Ni)	Formation of $\gamma\prime$ (Ni_3(Al, Ti)) phase, stabilization of face-centered cube (FCC) matrix, hinders the formation of deleterious phases
Cobalt (Co)	Increases the solvus temperature of $\gamma\prime$ and reduces the stacking fault energy
Chromium (Cr)	Solid solution strengthening, sulphidation and oxidation resistance, formation of grain boundary carbide
Iron (Fe)	Solid solution strengthening
Titanium (Ti)	Forms $\gamma\prime$ (Ni_3(Al, Ti)) and carbides (MC type) (where M= denotes a metal, M = Cr, Fe, W, Mo)
Aluminum (Al)	Forms $\gamma\prime$ (Ni_3(Al, Ti)) and enhances oxidation resistance
Carbon (C)	Carbide formation (Viz., MC, $M_{23}C_6$)
Boron (B), Zirconium (Zr)	Stress rupture property improvement imparts strength to grain boundaries.
Molybdenum (Mo), Tantalum (Ta), and Tungsten (W)	Strengthening of solid solution and carbide formation (MC type)
Lanthanum (La) and Yttrium (Y)	Improvement in oxidation resistance
Niobium (Nb)	Forms $\gamma\prime\prime$ (Ni_3Nb) and carbide formation (MC type)
Vanadium (V)	Forms $\gamma\prime\prime$

Table 2. Typical application of commonly used Nimonic superalloys.

Alloy	Applications	References
Nimonic 75	Engines of high-performance sports cars, gas turbine blades in the furnace for the heat treatment process, industrial thermal processing components	[23]
Nimonic 80A	Gas turbine components (discs, rings, blades), furnace, automotive exhaust valve, power units, manufacturing of fasteners, jet engines, die-casting inserts and cores, nuclear boiler tube supports	[24–26]
Nimonic 90	Turbine blades, discs, high-temperature springs, exhaust re-heaters, hot working tools, forging components	[27,28]
Nimonic C263	Gas turbine blades, power generators, heat exchangers, exhaust ducting, bearing housing, the combustion chamber of the gas engine,	[29,30]

scaling and oxidation resistance properties at high-temperature [16]. Nimonic 80A is an age-hardenable Ni and Cr alloy, strengthened by the addition of Ti, Al, and C, developed to work up to the 1088 K temperature limit. Nimonic 90 possesses good ductility and is suitable to work at temperatures up to 1193 K as 20% of Ni (in weight%) is replaced with Co. The addition of Co leads to an increase in the solubility temperature of γ' phase and increases carbon's solubility in the matrix, thus lowering the presence of carbide [17]. The Nimonic C263 superalloy was used in Rolls-Royce in the year 1971 as an alternative to Nimonic 80A in the sheet form with improved ductility [18]. Table 2 shows the typical applications of Nimonic superalloys, and Table 3 shows the chemical compositions.

The studies concerning the conventional and nonconventional machining of Nimonic superalloys are well-reported in the literature. Nimonic superalloys are capable of retaining the hardness even at higher temperatures and suppressing plastic deformation and chip formation. But, due to the low thermal conductivity of Nimonic superalloys, thermal stresses are induced in work and tool material (TM), leading to faster tool failure [19,20]. The built-up edge (BUE) formation is another problem in conventional machining of difficult-to-cut material, which leads to tool wear due to adhesion [21]. These problems in the machining of Nimonic superalloys have drawn the attention of researchers worldwide. These issues have motivated scholars worldwide to research non-conventional machining of Nimonic superalloys, viz., electrical discharge machining (EDM)/wire-EDM (WEDM), electrochemical machining, ultrasonic assisted turning (UAT), laser cutting, hybrid machining, etc. [22].

A total of 152 articles are considered in this review, out of which 91 articles are concerned with machining of Nimonic alloy. All the articles (journals, conference proceedings, and book chapters only) are original and peer-reviewed, extracted from Science direct, Springer, Google scholar, Scopus, SCI and Web of Science website. The number of papers published in recent years is shown in Figure 3. The figure shows that the average number of articles related to the machining of Nimonic superalloys is gradually increasing. Figure 4 shows the different techniques used for machining the Nimonic alloy i.e., 45% of EDM-related studies, 41.7% published articles on turning,

Table 3. Composition of different Nimonic superalloys [31].

Composition	Types of Nimonic superalloys			
	Nimonic 80A (in weight%)	**Nimonic 75** (in weight%)	**NIMONIC 90** (in weight%)	**NIMONIC C263** (in weight%)
C	0.10 Max	0.08–0.15	0.13 Max	0.04–0.08
Cr	18.0–21.0	18.0–21.0	18.0–21.0	19.0–21.0
Si	1.0 Max	1.0 Max	1.0 Max	0.40 Max
Cu	0.2 Max	0.5 Max	0.2 Max	0.20 Max
Fe	3.0 Max	5.0 Max	1.5 Max	0.7 Max
Mn	1.0 Max	1.0 Max	1.0 Max	0.60 Max
Ti	1.8–2.7	0.2–0.6	2.0–3.0	1.9–2.4
Al	1.0–1.8	–	1.0–2.0	0.60 Max
Co	2.0 Max	–	15.0–21.0	19.0–21.0
B	0.008 Max	–	0.02 Max	0.005 Max
Zr	0.15 Max	–	0.15 Max	
Pb	0.0025 Max	–	0.0020 Max	0.0020 Max
S	0.0015 Max	–	0.015 Max	0.007 Max
Ag	–	–	–	0.0005 Max
Bi	–	–	–	0.0001Max
Mo	–	–	–	5.6–6.1
Ni	Balance	Balance	Balance	Balance

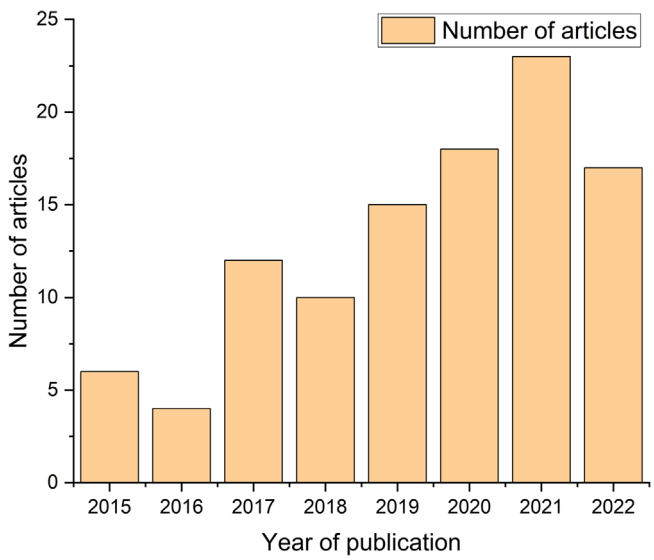

Fig. 3. Increase in the number of research studies on the machining of Nimonic superalloys

15.4% of articles on milling and remaining 15.38% of articles on other (drilling, UAT, electrochemical machining, hybrid machining) machining processes. The researchers widely studied the turning and EDM operations with respect to Nimonic alloys. Based on the literature review, the findings are summarized into different sections corresponding to the various machining techniques. The rest of the paper is organized as follows; Section 2 provide the details of the conventional machining of Nimonic alloys. Section 3 present the details of the non-conventional machining of Nimonic alloys. Section 4 summarizes the trends and scope for future work. Section 5 presents the conclusions.

2 Challenges in the conventional machining of Nimonic superalloys

The contribution by earlier researchers to the machining of Nimonic superalloys by turning operation is proportionately more compared to milling and drilling. Tool wear, surface roughness (SR), cutting force, and lubrication are the primary area of research in the case of conventional machining. The following sections explain the fundamentals of conventional machining (tool wear, SR, cutting force, and cooling), followed by the outcomes of turning, milling, and drilling of Nimonic superalloys in detail.

Knowledge of tool wear is crucial to enhance the tool life and thereby the productivity of the machining process. A worn-out tool will not only reduce the surface quality but also reduces the dimensional accuracy. The flank wear is considered as a conclusive factor in evaluating tool wear. It increases with an increase in cutting time and decreases with an increase in CS. In other words, the flank wear rate is significantly reduced at a higher CS when compared to increased cutting time. It is attributed to the gradual degradation of the cutting edge, which increases the contact between the tool wedge and the machined work surface. In machining of Nimonic superalloy, adhesion wear is the dominant tool wear mechanism at all CSs. Usually, tool wear starts at medium CS, and as the CS increases to a higher level, temperature also increases, and chemical and

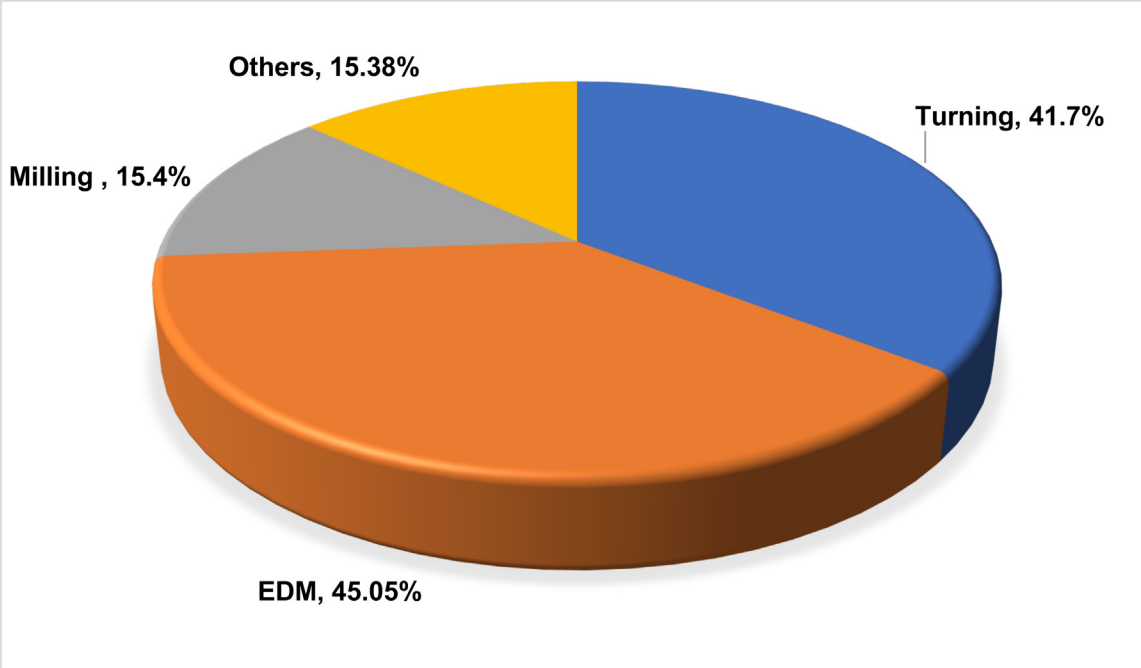

Fig. 4. Increase in the number of research studies on the machining of Nimonic superalloys

Table 4. TM used in the machining of Ni-based superalloy based on CS [32].

TM	CS (m/min)
Uncoated cemented carbide	20–50
Coated carbide	40–90
Ceramic	350–550
PCBN	250–400

diffusion wear become dominant resulting in failure of the cutting tool [32]. According to studies, the carbide inserts are found to produce better results while machining Ni-based superalloys within the average CS range of 45–55 m/min [33]. Table 4 shows some preferred tool materials and corresponding CS limits. It is observed that the friction between the tool and chip can be lowered by applying a specific coating on the cutting insert, thereby reducing the cutting temperature [34]. The cryogenically treated coated insert produces lesser flank wear during the machining of Ni-based superalloys because it resists adhesion and thereby prevents BUE formation. In the non-cryogenically treated coated insert, the formation of extreme BUE under the same cutting conditions is seen, which is attributed to the presence of a slightly longer chip-tool contact length, resulting in higher stress on the tool face, further leading to the failure of the principal cutting edge. Conversely, the cryo-treated inserts prevent the plastic deformation from resulting in fracture failure of the cutting edge due to the release of residual stresses [35]. During the machining of Ni-based superalloys, the temperature on carbide inserts reaches up to 1000 °C leading to BUE formation and chipping [36]. A good number of researchers have employed physical vapor deposition (PVD)-coated carbide inserts for machining Nimonic superalloys and observed varying degrees of success compared to chemical vapor deposition (CVD)-coated tools. Researchers have observed the formation of three distinct regions on the tool's rake face during the machining of superalloys: sticking region, sliding region and safer region. The sticking region is located near the nose, prone to chipping, chip adhesion and fracture. The sliding region is prone to coating peeling, abrasion, attrition, and striation marks, whereas the safer region is least affected by abrasion [37,38].

The SR is one of the commonly and widely used parameters to represent the quality of the machined surface. It depicts the amplitude and frequency of irregularities on the machined surface. The SR is affected by the cutting conditions, viz., CS, feed rate (FR), DOC, tool wear, work materials, cutting environment, and others. The final surface quality of machined parts influences tribological aspects like friction, wear, and lubrication in assembled parts. Thorough knowledge of surface finish will significantly help in deciding the right machining conditions and adequately monitoring the machining process.

Knowledge of the cutting force will help decide the power consumption, machine tool, and cutting tools. The magnitude of cutting force will be very high at a lower CS due to a higher coefficient of friction between the tool and work interface. However, as the CS increases, the temperature between the tool and work interface increases, softening the work and decreasing the cutting force [39].

Even though cutting fluids play a significant role in machining difficult-to-cut materials, dry machining is the best option from an environmental standpoint. Because

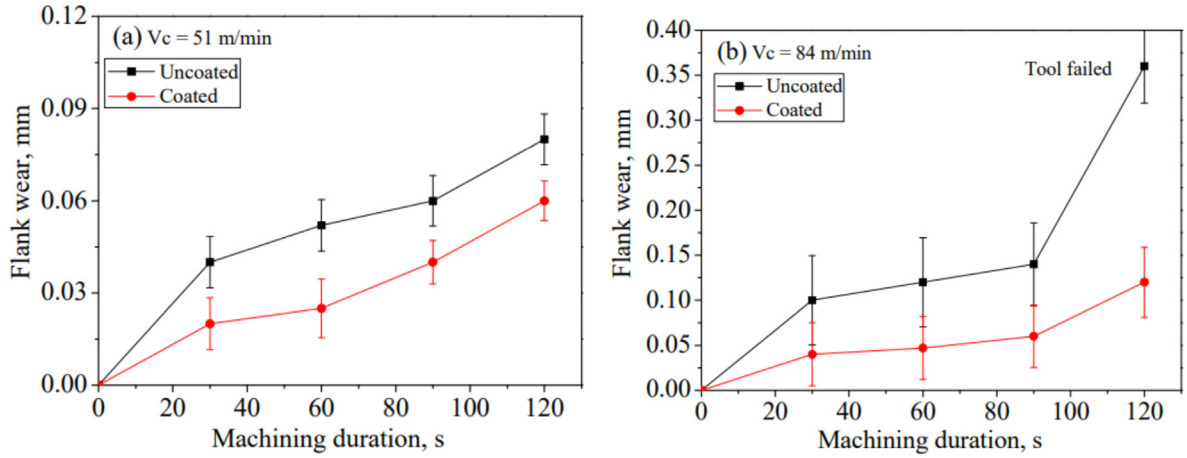

Fig. 5. Variation of flank wear rate with machining time for coated and uncoated insert at (a) CS = 51 m/min, (b) CS = 84 m/min [45]. Inderscience retains the copyright of the figure.

dry machining not only reduces the need for cutting fluids but also maintains the safety of the personnel. In addition to turning and milling, dry machining conditions can also be applied to a few other processes. However, dry machining is still not viable during the machining of difficult-to-cut materials due to a lot of heat being generated. Hence, much more research is required to eliminate the constraints and make dry machining industrially viable [40]. Flood cooling is very common in the metalworking processes. Conversely, flood cooling methods have limited usage despite cutting oils being cheaper, easily available and readily usable due to increased disposal costs and strict rules and regulations from government authorities. Further, improper disposal of cutting oils can cause water-oil pollution [7].

Hence, in recent times MQL method has been used in the machining process, which allows the limited quantity of a mixture of water and oil to get mixed at the cutting zone, thereby limiting the use of metalworking fluids and emulsion-based coolants. Additionally, oil drops play a vital role in the formation of tribofilm at the chip-tool interface [40]. However, few researchers have compared the effect of abundant cooling and MQL in the turning operation of Nimonic 80A and reported that abundant cooling has successfully enhanced the surface finish, volume of chip removal, and tool life compared to MQL [41].

The hardships faced during the machining of superalloys have eased considerably in the modern era with the increased usage of cryogenic coolants. The commonly used cryogenic coolants in machining processes are liquid nitrogen (LN_2) and liquid carbon dioxide (LCO_2). These cryogenic coolants successfully reduce the temperature generated during the machining process, but on the other hand, they will precool the work and thus increase the cutting force [1,42]. The LCO_2 and LN_2 boil at −78.5 °C and −198.79 °C under atmospheric pressure, respectively. When LN_2 is used as a cryogenic coolant, it lowers the cutting zone temperature to the point where it over-cools the workpiece, thereby causing the embrittlement of the material being machined and affecting the machining. Additionally, high cost, high expansion losses, and operator breathing problems during the machining operation are some other issues associated with LN_2. Hence, researchers differ in opinion on selecting LCO_2 and LN_2 as cryogenic coolants [43].

2.1 Turning

2.1.1 Studies on tool wear and SR

Singh et al. [44] investigated the wear behavior of AlTiN-coated and uncoated cutting tools during the turning of Nimonic C263 at the constant cutting condition (CS = 60 m/min, FR = 0.12 mm/rev and DOC = 1 mm). During the investigation, different tool inserts were used, viz., uncoated cemented carbide, coated cemented carbide, and coated cemented carbide with micro blasting. The key observations were that the uncoated insert failed faster than the coated insert, making it unsuitable for machining Ni-based superalloy. Secondly, in the uncoated insert, abrasion, adhesion, and diffusion wear mechanisms were dominant, whereas only adhesion and abrasion wear mechanisms were observed in coated inserts. Finally, the author has suggested using a micro-blasted coated cutting insert for enhanced tool life. A comparative study of the tool wear on coated ($TiN/TiCN/Al_2O_3/ZrCN$) and uncoated carbide inserts during the turning of Nimonic C263 has revealed that the uncoated tool failed sufficiently earlier than the coated tool. Figure 5 shows that at a higher CS (84 m/min), flank wear rate was high in the uncoated tool compared to that in the coated tool because of high-temperature generation at high CS, high mechanical stress, and the presence of hard carbide particles leading to abrasion wear. On the other hand, the coated inserts can provide higher thermal stability, antifriction, and oxidation resistance due to the presence of coating. Further, at a lower CS (51 m/min), the formation of BUE was observed on both coated and uncoated tools, mainly due to the higher chemical affinity of Ni, Cr, and Co present in the work material and higher coefficient of friction at the lower CS [45].

Another comparative analysis was performed on CVD and PVD-coated carbide inserts during the dry turning of Nimonic C263. The experiment results showed that PVD-coated inserts produced a better surface finish and

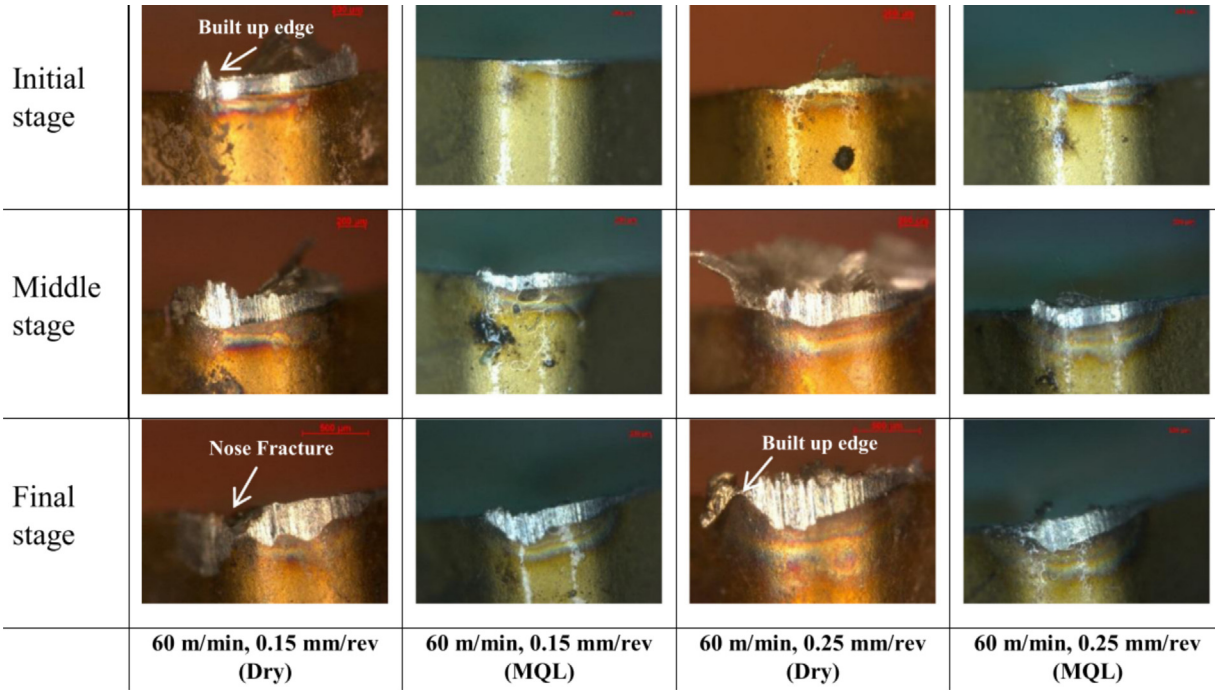

Fig. 6. Various stages in nose wear at different cutting conditions [36].

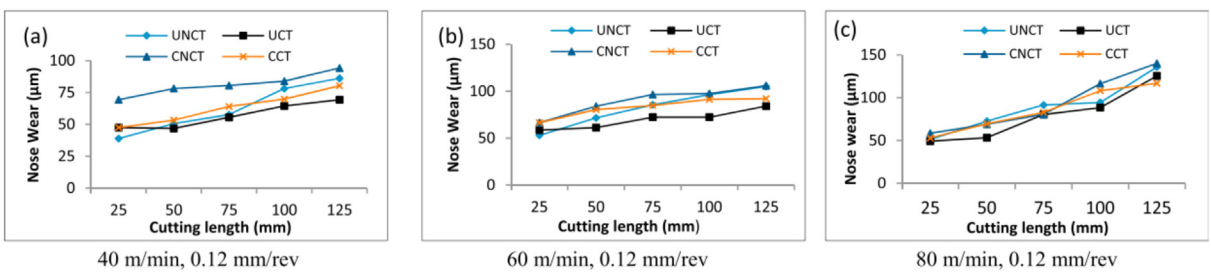

Fig. 7. Variation of flank wear on the nose side along with cutting length at (a) CS = 40 m/min, 0.12 mm/rev, (b) CS = 60 m/min, 0.12 mm/rev, (c) CS = 80 m/min, 0.12 mm/rev [35] (CNCT = coated non-cryogenically treated, CCT = coated cryogenically treated, UNCT = uncoated non-cryogenically treated, UCT = uncoated cryogenically treated).

better resistance to abrasion wear and underwent a lower flank wear rate at a lower CS. In addition, PVD coating produced better resistance to abrasion wear, whereas the CVD coating resulted in premature coating removal at a lower CS. However, the CVD-coated insert suffered a higher flank wear rate while machining at medium DOC and a lower FR. Analysis of variance analysis (ANOVA) concluded that the FR, DOC followed by CS, was the highest influencing factor on tool wear [46]. The machinability analysis of Nimonic 90 alloy under dry and MQL environments using a coated carbide insert as TM showed similar results. Increased FR and DOC increased SR, whereas SR decreased with an increase in CS for given machining conditions. The authors concluded that the DOC and FR were the most significant parameters in deciding the response than the CS [27]. However, according to Ezilarasan et al. [47], during the turning operation of Nimonic C263 alloy using PVD coated carbide insert revealed, the dominant factors for achieving lower value for tool wear were CS followed by FR and DOC.

Chetan et al. [36] conducted a turning operation of Nimonic 90 alloy using coated carbide insert (PVD TiN) and showed that significant tool wear occurs in the nose region due to fracture (Fig. 6), followed by sudden failure. Also, the amount of wear observed under dry conditions was more than that in the MQL condition. The mechanism of wear observed is abrasion wear. Further, the authors reported that the notch wear occurs mainly due to the adhesion mechanism and that the insert rake wear occurs due to coating peel-off, fracture, and edge chipping. In another study [35], the same authors evaluated the dry turning of Nimonic 90 alloy using cryogenically treated and non-treated inserts. The assessed findings highlighted that on an average the cryogenically treated insert outperformed the non-treated inserts by reducing the tool nose wear (Fig. 7). Also, a notable reduction in flank wear, cutting force and chip tool contact length were observed under cryogenically treated inserts. The increase in CS has resulted in an increase in tool wear due to an increase in temperature.

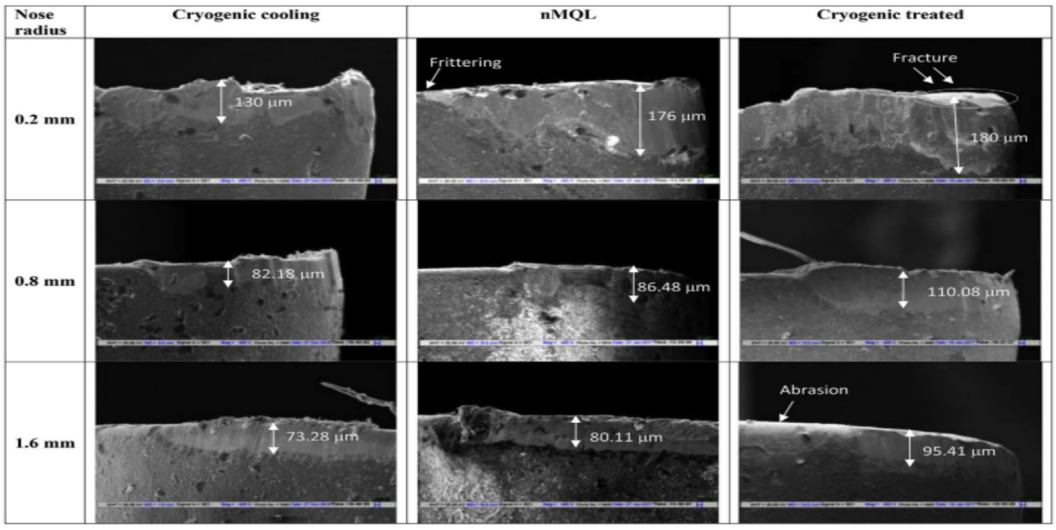

Fig. 8. Scanning electron microscope (SEM) images of cutting insert under different cooling conditions and nose radii at 60 m/min and 0.12 mm/rev [48].

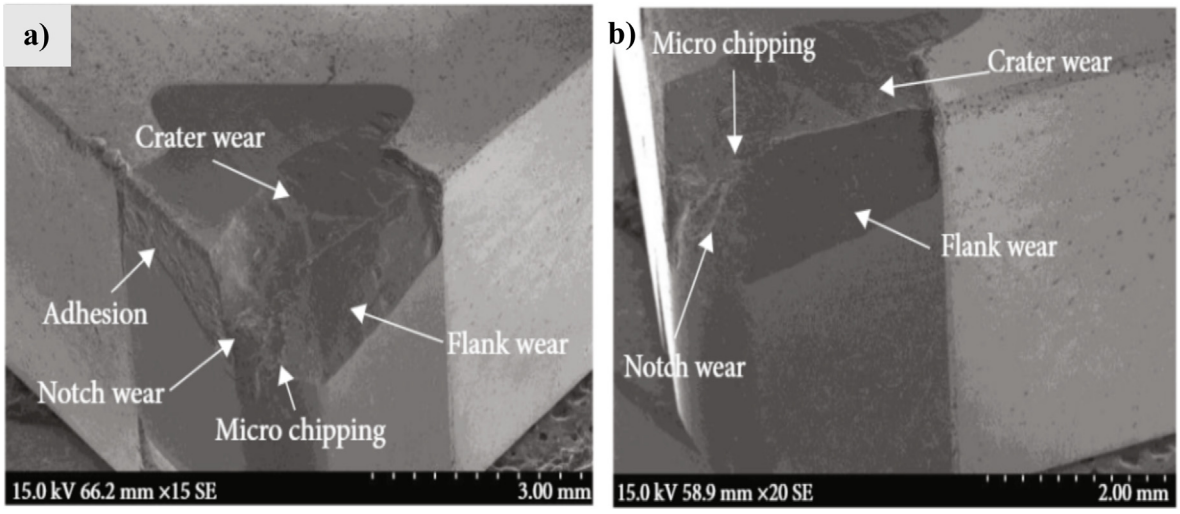

Fig. 9. SEM image of tool wear at (a) CS = 190 m/min, FR = 0.159 mm/rev, DOC = 0.75 mm. (b) CS = 190 m/min, FR = 0.096 mm/rev, DOC = 0.75 mm [49].

Further, the same authors compared the machining of Nimonic 90 alloy using coated tungsten carbide insert (AlTiN) of different nose radii under different cooling environments and reported the key observations. Firstly, the cryogenic environment was better followed by nanoparticle-based MQL (NMQL), as depicted in Figure 8. Secondly, cryogenically treated inserts performed better at higher cutting velocity under a dry environment. It was suggested to use larger nose radii inserts compared to smaller ones for better machining action [48]. Xavier et al. [49] studied dry turning of Nimonic C263 in terms of flank wear and SR using a cubic boron nitride (CBN) insert. FR was found to be the essential factor in cutting edge breakdown, followed by CS and DOC. The flank wear rate was 31% higher at higher CS and FR than at medium CS and low FR. Nevertheless, the SR values were reduced at higher CS, DOC, and lower FR. The main tool wear mechanisms observed were adhesion, abrasion, and micro-chipping, as shown in Figure 9.

Researchers have analyzed the tool wear during the dry turning of Nimonic 90 alloy using PVD coated (TiAlN) carbide insert for different cutting lengths viz., 50, 100, and 200 mm. Authors have noticed peel-off on the rake surface, corner nose wear, chip fragments on the principal cutting edge, notch wear on the auxiliary cutting edge, and breakage of the auxiliary cutting edge near the tool tip while turning operation on 50 mm length of the workpiece. On the other hand, chip adherence on the tool tip, notch wear, flanking, and BUE were observed on the auxiliary cutting edge while turning on the 100 mm length of the workpiece. Figure 10 shows the anomalies observed on the machined surface by the authors while turning on the

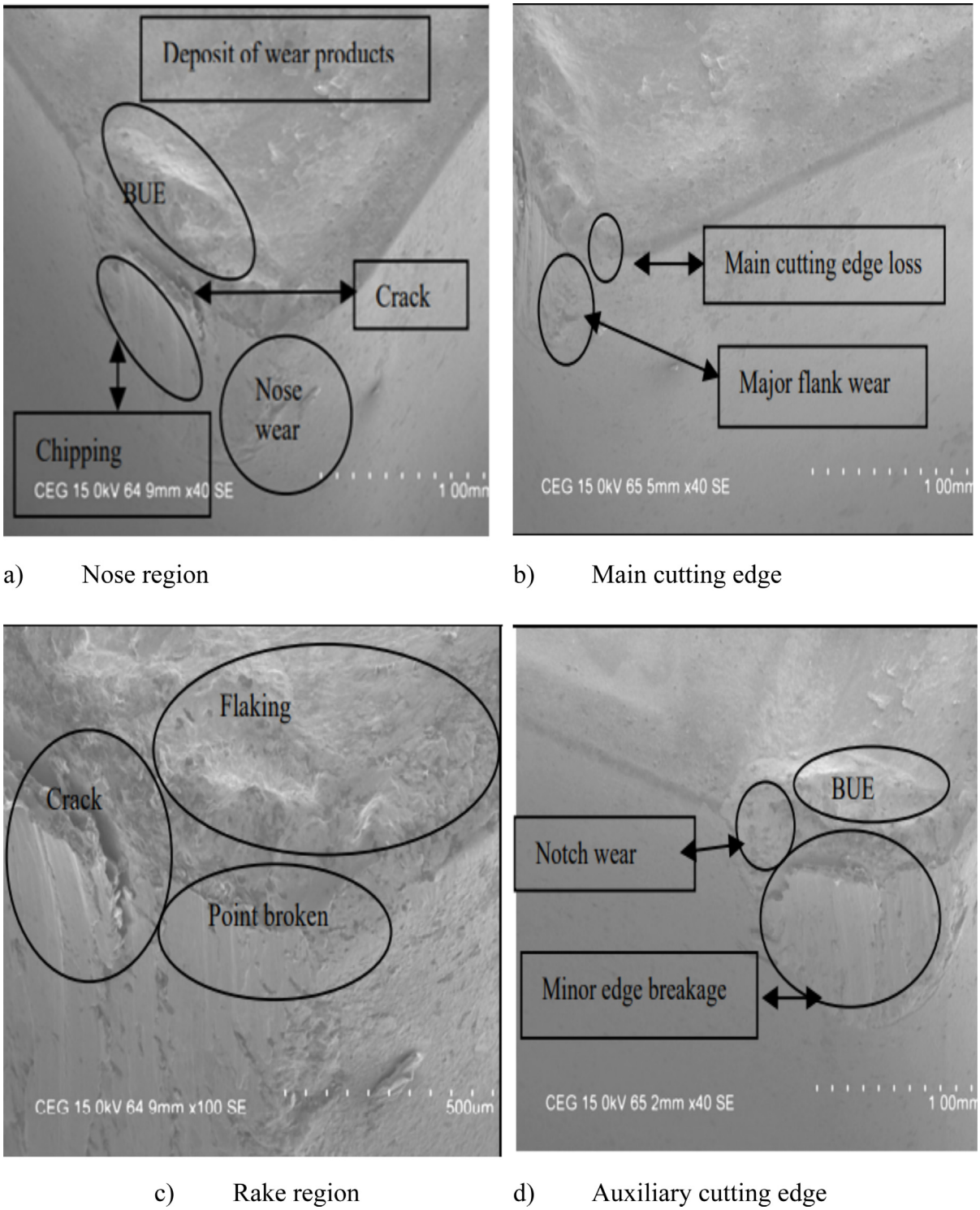

a) Nose region b) Main cutting edge

c) Rake region d) Auxiliary cutting edge

Fig. 10. Tool wear on (a) nose region, (b) main cutting edge, (c) rake region, (d) auxiliary cutting edge [50].

200 mm length of the workpiece, viz., BUE, chipping, deposition of wear products on rake face, notch wear, and nose wear [50].

The machined surface of Nimonic C-236 was evaluated under different cooling conditions (dry and wet) and cutting parameters using PVD multilayer-coated (TiN/TiAlN) and uncoated cemented carbide insert. The PVD-coated insert produced a better surface finish even under dry conditions than wet conditions (MQL and flood) using an uncoated insert. Authors credited the antifriction nature of coating provided between tool-work interface and retainment of sharp cutting edge for the same. Also, the SR increased with an increase in FR, attributed to the BUE formation and tool wear [51]. Ezilarasan et al. [29] analyzed the SR during the

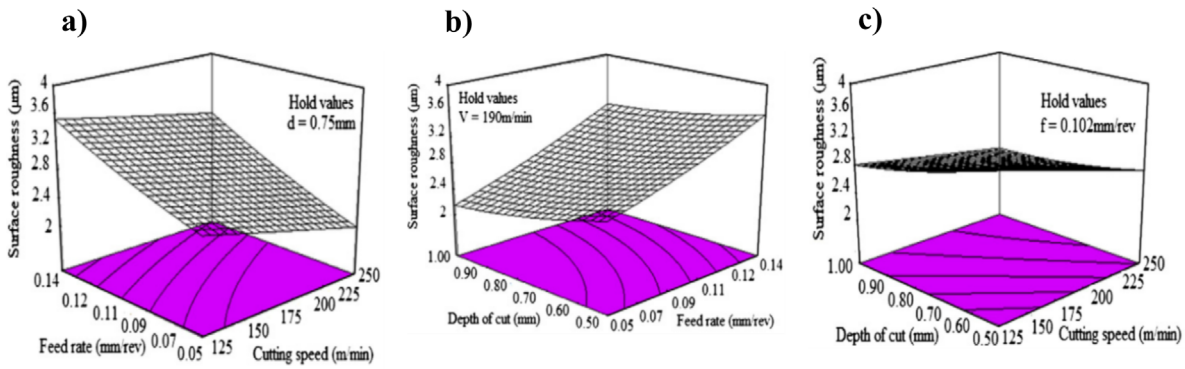

Fig. 11. (a–c) Variation of SR with cutting parameters [29].

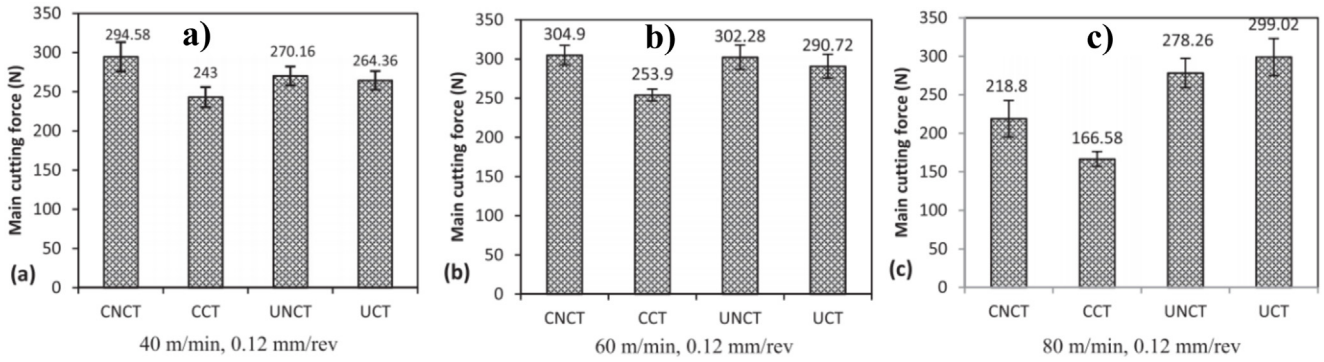

Fig. 12. Variation of cutting force with CS and FR (a) 40 m/min and 0.12 mm/rev, (b) 60 m/min and 0.12 mm/rev, (c) 80 m/min and 0.12 mm/rev [35] (CNCT = coated non-cryogenically treated, CCT = coated cryogenically treated, UNCT = uncoated non-cryogenically treated, UCT = uncoated cryogenically treated).

turning of Nimonic C263 under dry turning conditions using a whisker-reinforced ceramic insert. The experiments showed that SR was mainly influenced by FR than CS and DOC (Figure 11). The lower SR values were observed at a lower level of FR and at higher levels of CS and DOC.

2.1.2 Studies on cutting force

Chavan et al. [52] reported that the CS mainly influences tool wear and cutting force during the machining of Nimonic 80A using an alumina-based ceramic insert. It was recommended to go for medium FR and DOC and higher CS for dry machining of Nimonic alloy 80A using an alumina-based ceramic insert. Further, it was suggested that ceramic insets are well suited for Nimonic 80A alloy.

The usage of PVD-coated tools while machining superalloys has reduced the cutting force by 48% as compared to CVD-coated tools, attributed to the presence of Al_2O_3 coating in PVD-coated tools, which provides thermal stability, resistance to spalling, and wear. However, in CVD-coated tools, the presence of TiCN plays an important role in reducing the cutting force [46]. Venkatesan and Thakur [53] compared the machinability of Nimonic C263 alloy in terms of cutting force and SR. The superalloy was machined using PVD and CVD coated carbide insert at different CSs (60, 90, 120, 150 m/min), FRs (0.05, 0.12, 0.18, 0.25 mm/rev) and DOCs (0.4, 0.6, 0.8, 1 mm). A higher cutting force was observed at lower CS, higher FR, and vice versa. At lower CS, an increase in FR resulted in increased cutting force; however, increments in CS decreased the cutting force at all FR levels, attributed to the drop in shear strength and contact area. It was observed that an increase in FR and/or DOC increased cutting force. Authors have credited it to the increment of the primary and secondary shear zone. It has given rise to higher friction and thicker chips, leading to a higher material removal rate (MRR). Further, the authors noted that PVD inserts performed better than CVD inserts at a moderate range of FR. Authors in [35] recommended PVD coated-cryogenically treated insert for machining Nimonic 90 in terms of lower cutting force (Figure 12). The cutting force was notably reduced by 17% for coated cryogenically treated inserts than the nontreated inserts due to increased hardness and formation of eta-particles in the carbide matrix.

Ezilarasan et al. [39] analyzed the cutting force obtained during the turning operation of Nimonic C263 using a whisker-reinforced ceramic insert. The maximum cutting force of 850 N and 1100 N was recorded for a machining time of 9 mins at 125 m/min of CS, FR of 0.102 and 0.143 mm/rev, and a DOC of 0.75 mm. Authors have inferred that cutting force increases with an increase in FR, and at low CSs, cutting force was higher because of higher friction coefficient values at the tool-work interface. However, cutting force decreased with increased CS due to higher cutting temperature at the tool and work vicinity,

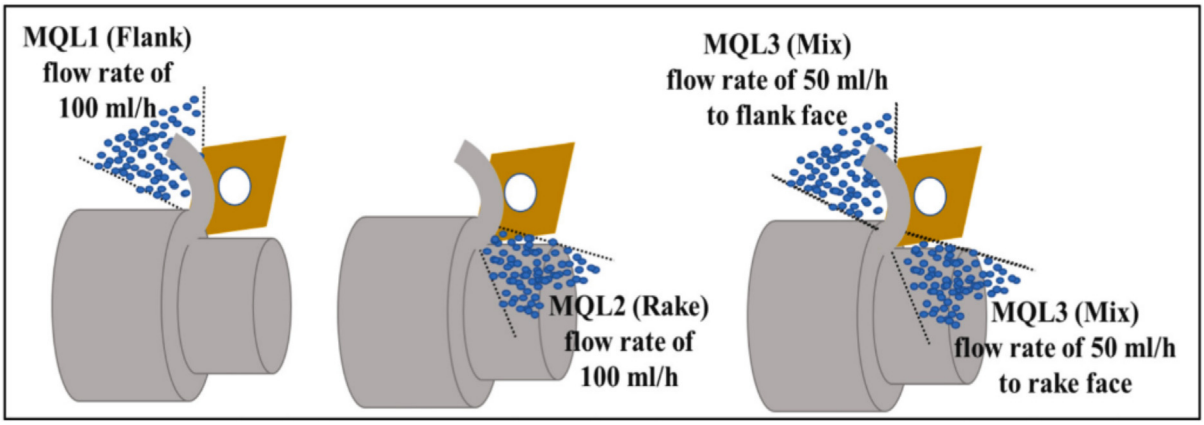

Fig. 13. Different positions of directing MQL [57].

leading to softening of the work material. The effect of cutting parameters on the cutting force during the turning of Nimonic 80A alloy was analyzed using both numerical and experimental methods. Researchers concluded that the DOC was the most dominant parameter in deciding the cutting and feed forces, with 48.4% and 80.14% contributions. In contrast, the FR was a dominant factor in determining the radial force, with a contribution of 83.15% from the ANOVA results. The simulated FEM model using Johnson-Cook (JC) parameters was successful in predicting the cutting force with a mean deviation of 6.45% [24].

The effect of cutting parameters on cutting force during turning under different cutting conditions was evaluated; the ANOVA analysis showed that the FR is a more significant factor in deciding the cutting force, followed by CS and nose radius. The increase in FR accelerates the MRR leading to thermo-mechanical fatigue and thereby increasing the cutting force. However, nose radius is a significant factor in deciding the thrust force followed by FR. But it was also observed that increasing the cutting-edge angle and maintaining a smaller tool nose radius results in a lower thrust force [48].

2.1.3 Studies on cooling and lubrication

The machinability of Nimonic 80A superalloy while undergoing a turning operation using coated carbide tool under dry, air, and oil cooling conditions was evaluated in terms of the tool wear. The authors [54] stated that oil spraying was the most efficient method for turning Nimonic alloy to achieve productivity using coated carbide insert. The best surface finish and tool life value were observed at 60 m/min CS under an oil-sprayed environment. NMQL (CuO nanoparticles mixed with groundnut oil) cooling condition used while turning Nimonic 90A using carbide tip showed that FR had a more significant influence on cutting force and SR whereas CS had no significant effect [55]. Researchers used MQL based cooling strategy to construct a specific cutting energy model for turning Nimonic 90. The strategy of applying MQL in the cutting zone with high pressure and flow rate resulted in reduced chip-tool contact length and shear flow stress over the rake face, reducing specific cutting energy [56]. Korkmaz et al. [57] investigated the influence of MQL and NMQL and the position of coolant impingement on the cutting insert (Figure 13) during the turning of Nimonic 80A using coated cermet insert. The proposed method resulted in a lower SR value for NMQL followed by MQL and dry conditions due to effective cooling and lubricating effect. Additionally, passing the cutting fluids in multiple directions resulted in lower tool wear and SR values. Kannan [58] investigated the turning of Nimonic 75 using neem and jatropha oil combined with hexagonal boron nitride nano particles (HBNNP). The experimental observation revealed 0.5 weight% of HBNNP in neem oil for sustainable machining and improved productivity. In addition, an increase in weight% concentration of oil and CS increased the SR, tool wear and cutting force.

A cryogenic environment was established by Jadhav et al. [59] to perform turning operations on Nimonic C263 using a cryogenically treated multilayer CVD coated (TiN-MT-TiCN-Al2O3 grade KCM25) cutting insert. The experiments showed that in the presence of cryogenic coolant, the SR diminished by 11%. In addition, nose wear and flank wear were found to be minimum. It was concluded that cryogenic holding time and cryogenic temperature were essential factors in deciding the SR. Particular research works by Patel et al. [43] employed LCO_2 coolant and flood coolant to investigate the turning operation of Nimonic 90 using a tungsten carbide insert. The experimental investigation uncovered that the cryogenic coolant increases the cutting force due to strain hardening, providing better chip breakability. In addition, the tool wear and power consumption were found to decrease under the action of the cryogenic coolant. However, cryogenic coolant failed to provide adequate lubrication, resulting in increased SR.

2.1.4 Studies on modeling techniques

Kumar et al. [60] worked on modeling and simulation using DEFORM 3D model to forecast the cutting temperature and force during the dry turning operation of Nimonic C263 alloy. It was observed from the statistical analysis that FR, CS, and DOC in specified order are found to be significant

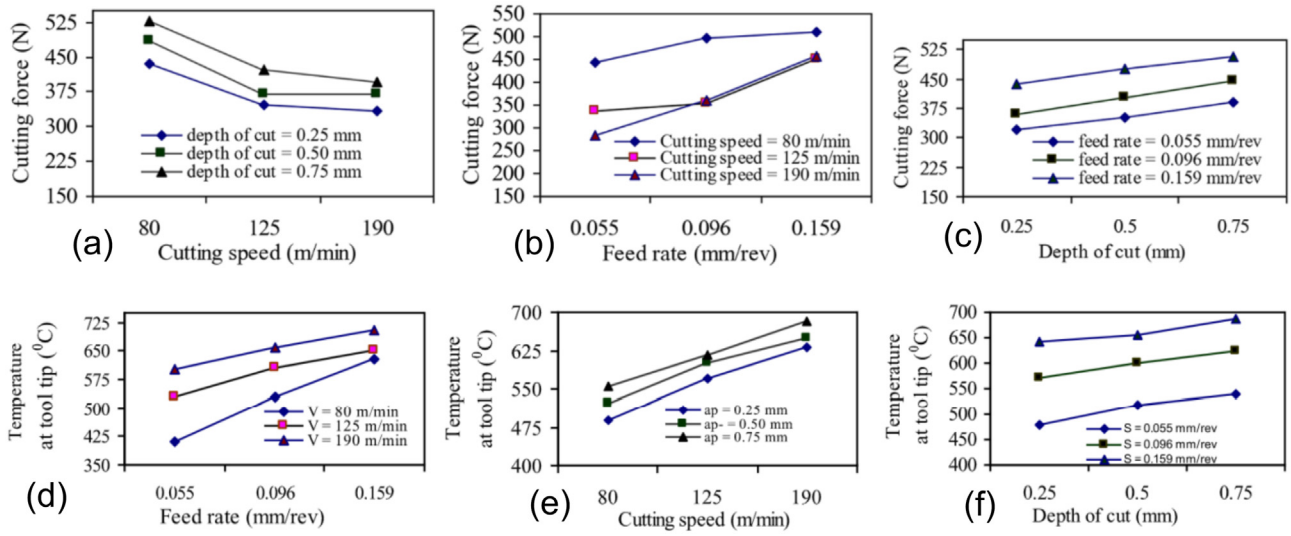

Fig. 14. Variation of cutting force along with (a) CS, (b) FR, (c) DOC; variation of cutting temperature at the insert tip with (d) FR, (e) CS, (f) DOC [60].

factors affecting cutting force and temperature at the insert edge. The cutting force was found to be higher at a lower CS of 80 m/min than at a higher CS of 190 m/min. However, as cutting parameters increased, the cutting tip temperature appeared to rise. Figure 14 shows the variation in cutting force and temperature along with the variation in cutting parameters.

The two-layer feed-forward artificial neural network (ANN) model was developed by Bose and Rao [61] to correlate the input and output parameters of turning operation on Nimonic 75 using coated carbide tool. The model results revealed that 35, 55, and 48.75 m/min were the optimum CS for obtaining minimum values of SR, cutting force, and temperature, respectively. Further, increased FR and DOC resulted in increased SR and cutting force but decreased temperature. Another study of similar nature by Ezilarasan et al. [62] was conducted during the turning operation on Nimonic C263 using PVD coated carbide insert, and the effect of different parameters were analyzed using response surface methodology (RSM). The analysis showed that FR was an essential factor influencing SR, followed by CS [62]. Ezilarasan et al. [63] used the Lagrangian finite element method with an orthogonal array arrangement of cutting conditions to develop an effective simulation model for the turning operation of Nimonic C263. The FEM model was used to predict the stress, strain, temperature at the tooltip, and the tangential cutting force. The results concluded that a maximum temperature of 620 °C was observed at the tooltip at 54 m/min CS, a 0.143 mm/rev FR, and a DOC of 0.75 mm. In addition, the maximum stress of 720 MPa was observed at a CS of 54 m/min. Krishna et al. [64] applied MOO based on ratio analysis (MOORA) and complex proportional assessment (COPRAS) combined with entropy for MOO of process parameters during the dry turning of Nimonic C263. The best experimental parameters from the optimization study were reported as CS = 125 m/min, FR = 0.055 mm/rev and DOC = 0.25 mm. FR was observed as the most significant factor in minimizing the cutting force and flank wear, followed by CS and DOC. Kumar et al. [65] used a wavelet-based histogram equalization technique to model the SR in the turning of Nimonic C263. The proposed noncontact type SR evaluation method was found to be effective, with a mean prediction error of 3.16%. Bommi et al. [66] proposed a novel FlankNet algorithm to evaluate the tool flank wear during the turning of Nimonic C263. The flank wear images were pre-processed, image features were extracted and a deep pattern model was used to predict the wear rate. An error of 3.03% between the predicted and measured flank wear values indicated the effectiveness of the proposed model.

2.1.5 Studies on residual stress

During machining, residual stresses develop on the surface or subsurface of the workpiece material due to thermo-mechanical loading. The material will be removed from the workpiece material due to severe plastic deformation upon the application of load. However, not all stresses generated during machining get relieved after the machining. Thus, the stresses that remain at the end of machining, especially at the free end of the surfaces, are known as residual stresses. Generally, the residual stresses are advantageous when they are in opposition to the imposed load [67]. Ezilarasan et al. [39] reported that CS and cutting time significantly influence the residual stresses developed during the machining of Nimonic C 263. Residual stress was found to be compressive when the tool was new. However, as the tool wears, the residual stress changed from compressive to tensile. Singh and Gangopadhyay [51] observed lesser tensile residual stress during the dry turning of Nimonic C 263 using coated carbide inserts. They also concluded that the coated inserts were ineffective in lowering the friction at lower FR.

2.2 Milling

2.2.1 Studies on Tool wear and SR

The responses of the milling process need to improve to achieve superior material characteristics at the lowest possible cost of production, as it is a critical material removal process for machining superalloys in industrial sectors such as aerospace [68]. In that regard, a research work reported that the milling cutter with a negative radial rake angle should be considered an option to achieve minimal tool wear and minimal specific energy consumption (SEC) while maintaining a high production rate in milling components of aerospace and high-temperature alloys. The authors revealed that the tool nomenclature had a significant effect on friction and frictional stresses than the cutting condition while milling Nimonic C263 alloy, and a similar result was also seen in the case of slot milling [69–71]. Ezilarasan et al. [72] examined the effect of cutting parameters in vertical milling of Nimonic C263 alloy using coated carbide tool. The SR was found to increase with grooves, chips, and feed lines at lower spindle speed and higher FR and DOC. Due to chipping and abrasion wear mechanisms, a similar trend was observed in the case of flank wear rate. Gowthaman and Jagadeesha [73] examined the effect of machining conditions on surface characteristics during slot milling of Nimonic C263 alloy. The authors concluded that table feed has the maximum influence on the surface characteristics, followed by the spindle speed and DOC. Furthermore, a reduction in table feed resulted in a significant decrease in the augmentation of compressive residual stress at constant DOC and spindle speed. In another study [74], the same authors examined the effect of dry, wet, and MQL cooling strategies on SR and cutting force. The ANOVA studies have shown that the cutting FR affects the cutting force, followed by the CS. However, due to their significant interactive outcome on SR, both FR and CS have similar effects on SR. The authors recommended the intermediate value of CS and FR at lower friction values, resulting in the formation of adequate lubrication, thereby reducing the temperature. Another key observation was that the MQL cutting environment provides a better finish to the machined surface at low power consumption [75]. In [76], it was reported that for a slot milling, tool with zero radial rake angle can be recommended followed by negative and positive radial rake angle tool to lower the tool vibration. Further, CS was found to have governing effect on the vibration amplitude followed by FR. However, in various machining conditions, the cutter with a positive radial rake angle invokes superior corrosion resistance, followed by cutters with zero and negative radial rake angle, which inhibit work surface corrosion [77].

2.2.2 Studies on cooling and lubrication

Adopting the MQL cooling strategy decreased the average SR by 47% during the milling of Nimonic C263 alloy using TiAlN-coated tungsten carbide. The authors attributed it to the penetration of the coolant at the tool chip interface, thereby decreasing the temperature at the cutting zone [78]. Research findings in [79] demonstrate that LCO_2 at the tool rake surface continuously lowers the machining temperature in the cutting area, thereby reducing the abrasion at the tool–work material junction and improving the surface finish. The compressive residual stress produced was more under LCO_2 conditions, thereby decreasing the flank wear by reducing the crack growth. The authors concluded that applying the cryogenic coolant during the milling of Nimonic 80A is the prime reason (using PVD-coated tungsten carbide) to achieve a better surface finish. However, wet and MQL-based machining produced similar SR values but at higher CSs. Further, MQL mist penetrability was low during the machining of superalloys due to the higher temperature in the machining area leading to increased SR. The authors reported that the cryogenic cooling successfully reduced the SR by 42–47%, 24–27% and 16–21% when compared to dry, wet and MQL cooling strategy respectively.

A high-pressure cooling system operated at 50 bar enhanced the performance parameters during the milling of Nimonic C263 using coated (TiN/TiAlN) carbide insert. The tool life was increased by 133% under a high-pressure coolant. On the other hand, using a cryogenic-based coolant during the machining was unfavorable as it increased the chipping of the cutting insert and the hardening of the work material [80]. However, in another research work [81], a nozzle containing the cryogenic coolant (LCO_2) was tilted at 45° to the Bilayer PVD-TiAlN/TiN-coated carbide insert during the machining of Nimonic-80A, thereby revealing the positive effect of cryogenic coolant on the machining. The experimental results showed that the cryogenic coolant effectively decreased the SR by 38–45% and 13–18% compared to the machining under wet and MQL conditions, respectively. In addition, the cryogenic coolant curtailed the tool-chip contact during milling, reducing the flank wear rate by 28–43% and 15–23% compared to the machining under wet and MQL conditions, respectively. The tool wear mechanisms, namely, abrasion and adhesion, were less prevalent under cryogenic cooling when compared to the conventional cooling strategy. Nevertheless, the compressive residual stress was more on the machined surface under cryogenic cooling conditions [81].

In a continued study on cryogenic machining during the milling of Nimonic 80A, Ross et al. [1] introduced a hybrid cooling system using PVD-coated TiAlN carbide insert and successfully enhanced the surface attributes and tool life. In the hybrid cooling, a combination of LCO_2 and MQL was directed toward the tool cutting edge. The hybrid cooling system reduced flank wear by 48–71%, 42–56%, and 22–40% compared with flood cooling, MQL, and LCO_2 alone. Figure 15 shows the wear on inserts under various cooling strategies. However, the residual stress and microhardness were found to be more under the cryogenic-based cooling approach. Figure 16 shows SR variation under different cutting conditions from the same study reported in the article [82]. In another study, researchers effectively machined the Nimonic 80A under the hybrid cooling system with lesser tool wear, SR, SEC and temperature. The increase in CS caused the workpiece to soften, lowering the SR value. On the other hand, increased FR caused the chatter to increase, which increased the SR. Conversely,

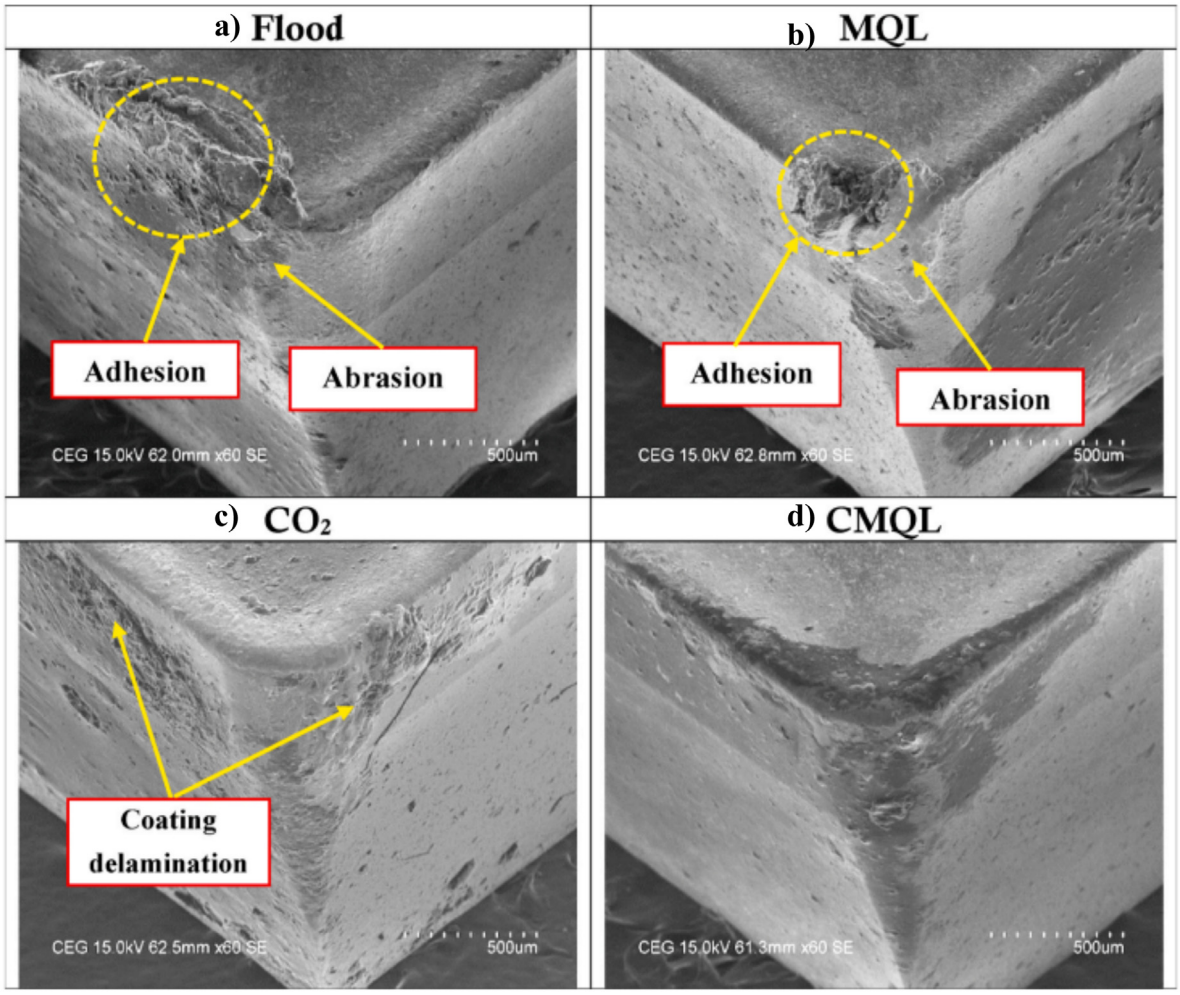

Fig. 15. SEM images of tool wear for (a) flood, (b) MQL, (c) LCO_2 and (d) hybrid cooling conditions (CS = 60 m/min, FR = 0.04 mm/rev) [1].

research studies on simulation and analytical models that consider hybrid cooling conditions in the machining of superalloys are still unavailable. As a result, there is ample scope for research to develop models that predict the hybrid cooling conditions in the machining of superalloys [83].

2.2.3 Modelling studies

Hassanpour et al. [84] evaluated the process parameters of end milling on Nimonic 115 using coated carbide tool through RSM and ANOVA analysis. The FR and the axial DOC were found to be the most and least significant factors affecting the SR, respectively. In another study [85] on the end milling of Nimonic C263 using coated (TiAlN) tungsten carbide insert reported that the radial rake angle of the tool had a significant role in deciding the SR, followed by FR and spindle speed being the least affecting factor. Further, in [86], researchers achieved superior surface characteristics by increasing the FR to 10 mm/min and spindle rotational speed to 78.5 m/min. The variations in the skewness and kurtosis values proved that the tool nomenclature, followed by the interaction effect between spindle speed and tool FR had a significant influence on the end milling of Nimonic C263. The key recommendation from the research was that a tool with a negative rake angle and tool feed of 7 m/min improved the surface parameters by 20% when compared to other machining parameters.

2.3 Drilling

The drilling operation on Nimonic C263 using AlCrN coated drill under silver NMQL showed that the optimum coolant pressure and nanoparticle concentration values were 750 kPa and 1.5 g (weight%), respectively. The authors concluded that the FR followed by the CS, the concentration of nanoparticles, and the coolant pressure was the order of importance in deciding the tool wear. It was also reported that the temperature and the SR increased with a lower coolant pressure and nanoparticle concentration [87]. Nagaraj et al. [88] developed a FEM-based simulation model to predict the force and temperature generated during the drilling of Nimonic C263 using a coated carbide drill bit. The study concluded that the temperature distribution at the cutting-edge increases with an increase in point angle and spindle speed. In addition, effective stress and strain in the cutting zone increased

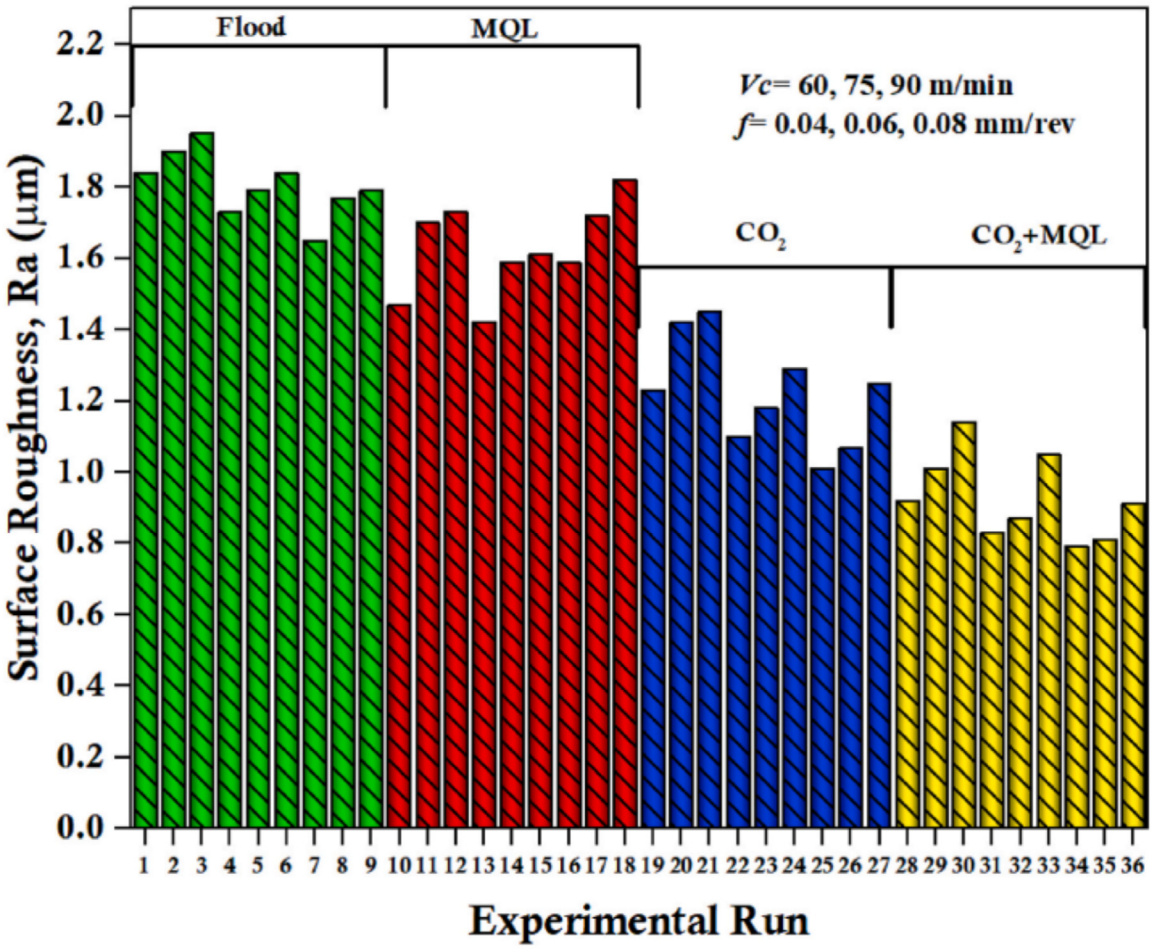

Fig. 16. Variation of SR under different cutting conditions (CS = 60, 75, 90 m/min; FR = 0.04, 0.06, 0.08 mm/rev) and cooling strategies during end milling of Nimonic 80A [82].

proportionately with spindle speed, FR, and point angle. Kumar et al. [89] developed a neural network for predicting responses during dry drilling of Nimonic C263. An error within 5% was observed during the prediction of SR and cutting force using the developed model. Further point angle was reported as the most significant factor affecting SR, followed by CS and FR. However, CS was the dominant factor in cutting force, followed by point angle and FR.

2.4 Summary of conventional machining

Researchers have shown greater interest in exploring the knowledge of turning Nimonic alloys. The various study areas include comparing coated and uncoated inserts, analysis of various types of inserts, analysis of tool wear patterns, analysis of SR, tool wear and cutting force, comparing dry and wet turning, comparing different cooling strategies, modeling studies and study on residual stresses. Among all the studies modeling studies and studies on residual stresses are very limited. Furthermore, studies need to be conducted on residual stresses, modeling and optimization techniques and the dimensional accuracy of parts to fill the research gap on the same. Most of the research proved that coated inserts are better for turning Nimonic alloys. The presence of coating will inhibit material removal from the insert, thus expanding the tool life. Many studies have suggested PVD-coated inserts for turning Nimonic alloy; this is in accordance with [90]. Further, many studies have adopted coated carbide inserts for turning Nimonic alloy and observed favorable results. Adhesion and abrasion are prominent tool wear mechanisms reported and BUE, chipping, notch formation, flank wear, rake wear, and nose wear are commonly observed wear patterns. Among the cutting parameters (CS, FR and DOC), FR significantly affects the overall turning operation performance. SR of machined components is very essential as it decides the tribological characteristics of the same in the assembly. Thus, researchers have paid greater interest in analyzing the SR and enhancing the surface quality. Thus, it is recommended to go for finish turning after rough turning. Relatively higher CS, and medium FR and DOC yielded comparatively better surfaces. From an economical and ecological point of view, dry or MQL machining is most beneficial. However, if dry machining is not feasible in terms of productivity and reliability, MQL machining can be effectively used. The use of cryogenic machining and cryogenic treatment of inserts have resulted

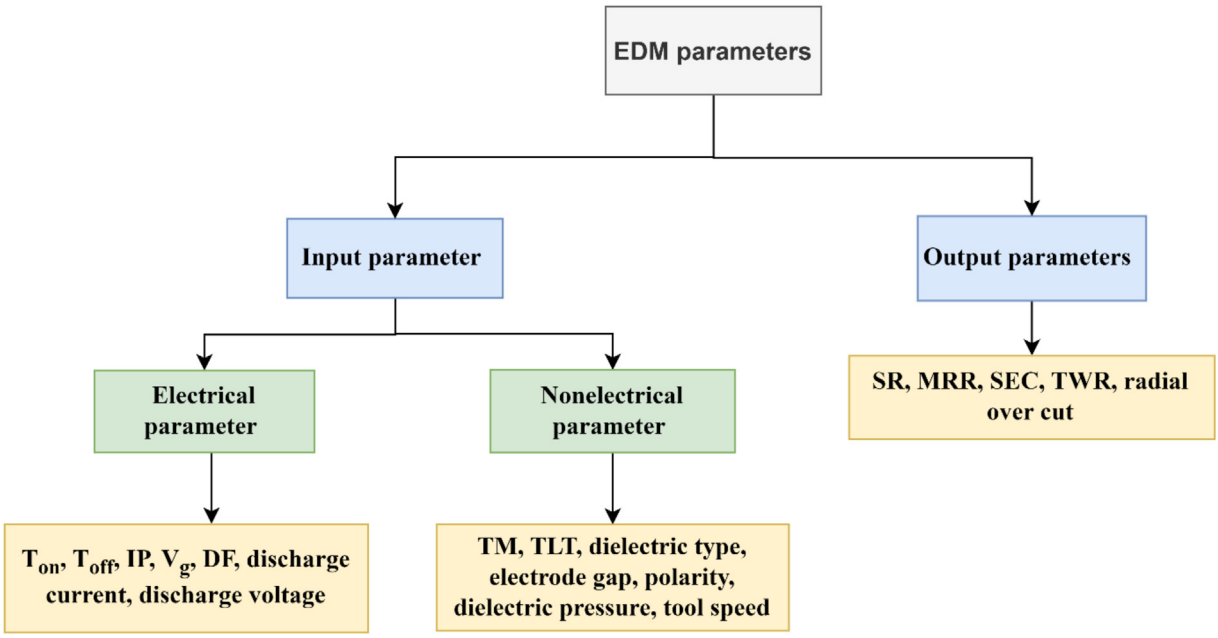

Fig. 17. Input and output parameters of EDM (T_{on} = pulse on time, T_{off} = pulse off time, IP = peak current, V_g = gap voltage, DF = duty factor, TM = tool material, TLT = tool lift time, SR = surface roughness, MRR = metal removal rate, SEC = specific energy consumption, TWR = tool wear rate).

in positive tool wear and SR results. Nevertheless, its cost-benefit analysis and mechanism through which it will lubricate the machining process need to be defined.

Compared to turning, studies on milling are very limited. Mainly, the authors have focused on evaluating responses in end milling and slot milling operations. Evaluation of tool wear and SR, comparison of different cooling strategies and statistical analysis are some of the main areas of study in milling. Most studies employed coated carbide tools for milling. FR is found to be a more dominating parameter influencing the milling responses among the cutting parameters. The use of MQL and cryogenic cooling have positively impacted the responses of milling. Hybrid cooling is a relatively new cooling strategy, and further studies are required on it. As different studies on milling focus on different objectives, summarizing the general opinion is very tedious. Furthermore, studies on milling are required to address the knowledge gap on modeling and optimization, cryogenic induced residual stress, different wear patterns and wear mechanisms, dry or near dry (air) machining, hybrid cooling, etc.

The availability of literature on the drilling of Nimonic alloy clearly indicates that research studies on Nimonic alloys are yet to be addressed. Also, to the best of the authors' knowledge, no reportable studies are found on the grinding of Nimonic alloys.

3 Challenges in the non-conventional machining of Nimonic alloy

Non-conventional machining methods are becoming increasingly common due to their ability to cut complicated workpieces. Advanced machining techniques are often used to create complex shapes. The criteria include low tolerance, good surface finish, and high production rates. The popular nonconventional methods used for machining Nimonic alloys include EDM and WEDM and, to a lesser extent, electrochemical milling, laser cutting, UAT, EDM-based drilling and EDM-based grinding, etc.

EDM is one of the prominent nonconventional machining processes introduced in the late 1940s, used in the machining of conductive hard-to-cut materials like Ni-based alloys, Ti-alloys, low alloy steels, Co-based superalloys, and ferrous-based superalloys to manufacture dies, molds as well as to finish the parts of surgical components, aerospace, automotive parts. In EDM, the electro-thermal energy conversion principle is used, wherein the material is removed through the formation of a spark [91]. Dielectric materials (water-based, gaseous-based, hydrocarbon-based) were used during the EDM process to alter the sparking trend, thereby enhancing the performance of the machining process in terms of surface finish and MRR [22]. In addition, EDM is a noncontact machining process due to which the tool impression on the work material, tool vibration during machining, and mechanical stresses are eliminated [92]. Die-sinking EDM (EDM) and WEDM are the two types of EDM processes widely used in machining Nimonic superalloys. In die-sinking EDM, a mirror image of the tool is produced on the workpiece. Figure 17 shows EDM electrical and non-electrical input parameters [93].

On the other hand, WEDM has become a more versatile machining technique in the turbomachinery industry to produce turbine engine parts in the current years [92]. In WEDM, a continuously moving vertical wire under tension acts as an electrode that removes the material through melting and vaporization. The input parameters are the

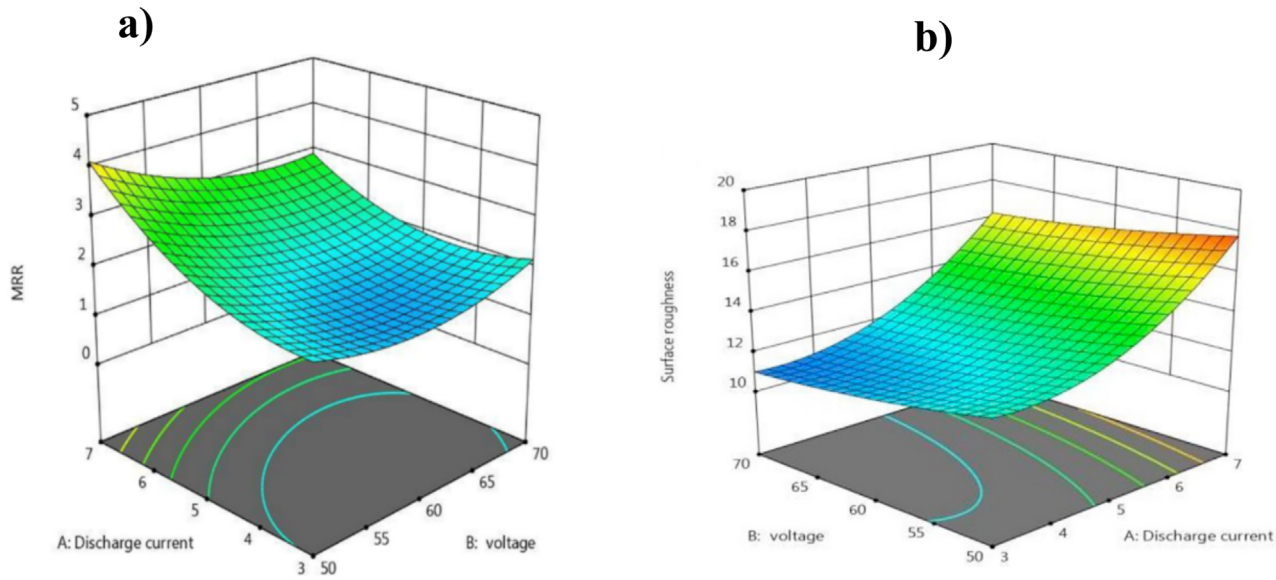

Fig. 18. Variation of (a) MRR with discharge current and gap voltage (V_g). (b) SR with V_g and discharge current [96].

Pulse on time (T_{on}), pulse off time (T_{off}), peak current (IP), and wire feed, whereas MRR, SR, kerf width, and kerf taper are the responses evaluated usually during WEDM [94].

3.1 Literatures on EDM of Nimonic alloy

The primary goal of process monitoring and control is to limit the deviation of performance measures from the intended level by observing and measuring process parameters, followed by continuous monitoring and tuning of the process parameters to acquire the desired response. Shastri and Mohanty [95] found that the Cu-electrode exhibits better performance when compared to the W and Cu-W electrodes with the lower SEC in the EDM of Nimonic C263. The electrode wear rate was significantly affected by electrode material and discharge current. The results showed that the Cu-electrode outperformed the other two based on electrode wear rate. However, the discharge current affected the SR, causing the W-electrode to consistently produce a superior machined surface among the three electrodes. A lower discharge current during the EDM of Nimonic C263 produced an accurate and precise cut. But an increase in discharge current resulted in the increased spark energy leading to a more significant amount of material being removed from the work material, thereby producing an asymmetric surface. The variation of MRR and SR with process parameters was depicted in Figure 18. The authors suggested that the W-electrodes could be used to make EDM parts that were precise and reliable [95,96]. A similar type study by [97] compared the effectiveness of Cu, brass, and W-electrodes during machining Al-powder mixed EDM of Nimonic 75. The authors reported two significant findings: the brass electrode provides a better SR despite a higher tool wear rate and the Cu-electrode had a higher MRR. On the other hand, the performance of the W-electrode was in between that of Cu and brass electrodes. However, in [98], the W electrode produced more finely machined surfaces than Cu and Cu-W electrodes. The SR of the machined surface indicated an upward trend as the T_{on} and IP increased. But the entire machining cost for the Cu electrode was reported as lesser. The IP was found to be the most important factor with a contribution of 60.29% in deciding the overall cost of the machining. Vivek et al. [99] introduced laser hardening and plasma nitriding and a combination of both (duplex method) on graphite electrodes in EDM of Nimonic 90. The duplex method produced graphite electrodes with 54% higher hardness than the other methods. Additionally, the duplex method reduced frontal and lateral wear by 49% and 42% for graphite electrodes. The pulse duration has made a significant contribution to improved electrode wear. Dewan and Kundu [100] studied powder (Ti) mixed EDM of Nimonic C263 and reported the highest MRR at IP = 10 mA and powder concentration = 9 g/L. However, the least SR was reported at IP = 8 mA and powder concentration = 9 g/L. IP was discovered to be the response-dominating parameter, followed by powder concentration, flushing pressure, T_{on} and T_{off}.

Choudhary et al. [19] reported that the negative polarity electrode used in the EDM of Nimonic 75 produces a much better surface finish than the positive polarity due to less material being removed by the negative polarity tool (Figure 19). However, due to its high erosion rate, a large amount of Cu deposition was observed on the machined surface. On the other hand, tools with positive polarity removed a large amount of material in the form of shallow craters, whereas unremoved material solidified to form recast layers. Thus, a higher deposition of materials was observed on the machined surface. In addition, the presence of carbon content was slightly more due to the higher dielectric pyrolysis rate in the positive polarity tool. According to [101], IP and aspect ratio were the main factors responsible for decreased SR and electrode wear rate and increased MRR during EDM of Nimonic 75 using the disk-type Cu- electrode. The disk electrode with a

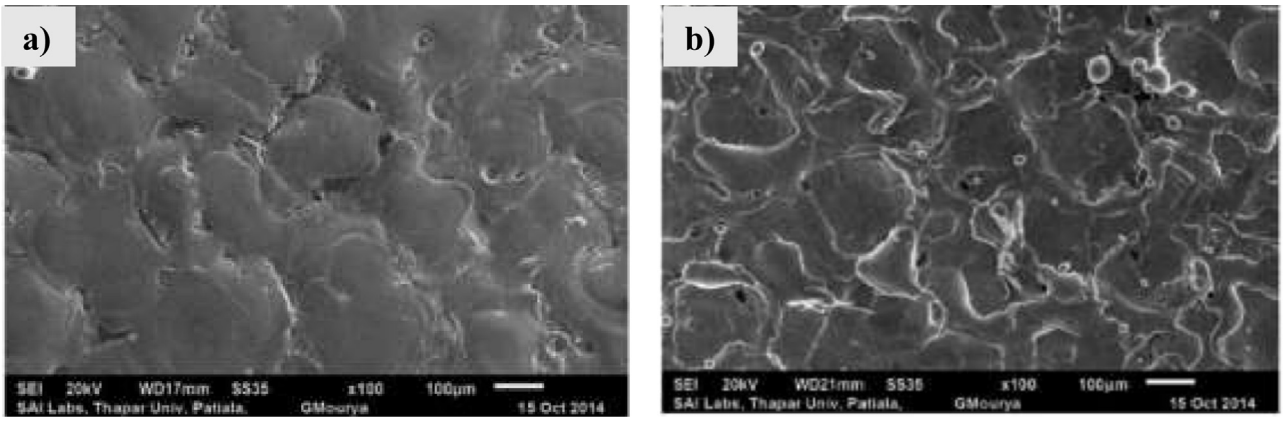

Fig. 19. Machined surface images using (a) negative polarity electrode, (b) positive polarity electrode [19].

greater aspect ratio and bigger surface area resulted in easier heat removal during each pulse duration, thus lowering the electrode wear rate. Authors have also reported that the rotation of the disc electrode aids in the effective removal of debris due to centrifugal force, which forces the dielectric fluid and debris outward.

Sahu et al. [93] conducted EDM experiments on Nimonic 80A and observed carbon transfer due to the decomposition of the dielectric and Cu on the workpiece surface. Authors reported that an increase in either IP or T_{on} results in a faster rate of material removal and a faster rate of tool wear. Further, the re-solidification of molten debris and deposition of worn-out electrode material on both the work and tool surface affect the MRR and the tool wear rate. The authors stated that the intensity of crack formation and supplied input energy sources were directly proportional to each other.

Chekuri et al. [102] predicted the process parameters of EDM of Nimonic C263 with the Cu-electrode by employing regression and ANN models. The analysis showed that IP was the most significant input parameter affecting the output parameters, viz., electrode wear rate, material erosion rate, SR, and dimensional overcut, followed by T_{on} and T_{off}. Further, out of all the ANN architectures, the 6-6 architecture had a remarkable prediction accuracy of 99.71%, compared to 93.55% for regression analysis. The same authors in [103] developed a multi-regression model to predict the responses of EDM of Nimonic C263 superalloy using fine-grained graphite electrodes. After analyzing SR, tool wear rate (TWR), MRR and radial overcut, the authors noted that the MRR and TWR were directly proportional to IP and T_{on} under optimum conditions. Conversely, T_{off} yielded the opposite result. The authors also noted that the SR tends to decrease with increased T_{off}, whereas the effect of the flushing pressure on the TWR was found to be insignificant. Another group of researchers conducted EDM of Nimonic 75 using Cu as well as a brass electrode and performed MOO of the responses viz., MRR, and SR. The authors used both regression model and teaching-learning based optimization method to obtain the optimized values of IP, V_g, T_{on}, T_{off} and lift time as 6 A, 50 V, 200 µs, 90 µs, 2 s, and 12 A, 40 V, 120 µs, 15 µs, 2 s for Cu and brass electrode respectively [23]. In [104], the authors reported the optimum process parameter values, viz. T_{on}, T_{off}, IP, and tool rotation on the responses viz., SR, electrode wear rate, overcut, and MRR for EDM of Nimonic 90 were 100 µs, 75 µs, 14 A, and 925 rpm, respectively. The authors observed that the IP was the most influential process parameter.

3.2 Literatures on WEDM of Nimonic alloy

Goswami and Kumar [105] reported a strong relationship between the input energy supplied and the surface integrity in the WEDM of Nimonic 80A. The supply of low input energy resulted in a comparatively better finish to the machined surface. Still, the supply of high input energy resulted in a rough surface with deep holes and a bunch of BUE layers, as depicted in Figure 20a and 20b. Additionally, the presence of a thinner recast layer deposition at lower input energy can also be observed in Figure 20c and 20d. The authors concluded that a supply of high input energy vaporizes a large quantity of metal and re-solidifies a small amount of metal to form thicker recast layers. A similar observation was reported during WEDM of Nimonic C263 in [20]. The authors highlighted that the SR and the cutting rate were directly proportional to the IP and the spark energy and inversely proportional to the spark frequency.

Singh and Misra [106] applied ANOVA and RSM to identify the significance of various process parameters viz., T_{on}, T_{off}, IP, and servo voltage on the CS during the WEDM machining of Nimonic C263 superalloy using a half-hard brass wire tool. The authors observed that T_{on} was the most significant process parameter influencing the CS, followed by the IP. The T_{off} and servo voltage were found to be less effective. Based on all the observations, the authors concluded that the CS is directly proportional to the IP as well as the T_{on} and inversely proportional to the T_{off}. Further, the process parameters were also found to have an interaction effect on the CS. A study involving cryogenically treated brass wire during WEDM of Nimonic 80A showed that an increase in the IP results in a rise in the MRR and a decrease in the SR. However, the FR had no significant effect on the MRR and the SR [107].

Jangra et al. [108] compared the trim and rough WEDM on Nimonic 90 and other superalloys at different discharge energies. The trim cut was performed after the rough cut with a higher level of discharge energy and higher

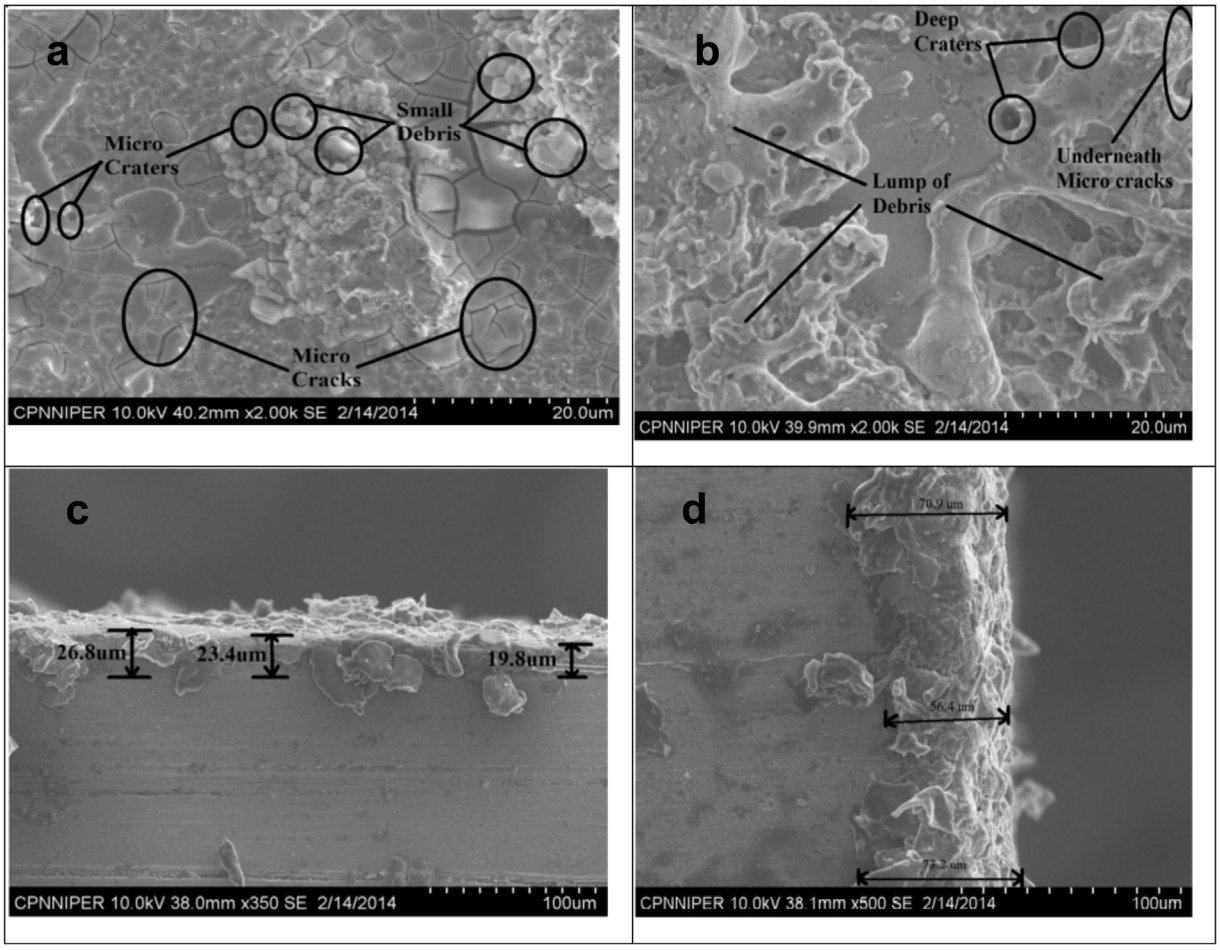

Fig. 20. Showing SEM images during WEDM of Nimonic 80A of (a) surface at low input energy, (b) surface at high input energy, (c) recast layer at low input energy, (d) recast surface at high input energy [105].

wire offset, resulting in an improved surface finish. The authors observed that increased discharge energy led to increased machining speed. Higher SR was attributed to the high rate of heat generation and work material evaporation, as depicted in Figure 21. Hence, the authors concluded that the SR could be decreased with a single trim cut, low level of discharge energy, and lower wire offset [108].

Mandal et al. [109] suggested a post-processing method after carrying out the WEDM of Nimonic C263 due to the thermal erosion mechanism occurring in the WEDM, which produces micro-cracks and voids that affect the material surface quality and mechanical characteristics. Additionally, the diffusion of elements into the machined surface from the dielectric as well as an electrode, along with the vulnerability of the machined surface to high-temperature oxidation, causes high-profile deviation. Hence, the authors proposed to carry out grinding followed by etching as the multi-cut post-processing method after the rough and finish cut by WEDM to remove the recast layers, thereby enhancing the surface asymmetry. The authors claimed that the proposed multi-cut post-processing method could restrict SR to as low as 0.024 µm.

Singh and Misra [110] developed an empirical model of wear ratio during the WEDM of Nimonic C263. The effect of various process parameters viz., T_{on}, T_{off}, servo voltage, and IP on the wear ratio was analyzed. The maximum wear ratio was achieved at the optimum values of T_{on}, T_{off}, servo voltage, and IP at 107 µs, 57 µs, 59 V, and 78 A, respectively. Authors claimed that the developed model could predict the wear ratio with an error of 1%. Further, the T_{on} was found to be a significant factor in affecting the wear ratio with a confidence level of 95%, as presented in Figure 22.

Kumar et al. [111] developed an SR model for WEDM of Nimonic 90 superalloy by combining a mathematical model of RSM with a genetic algorithm. The authors found that the minimum SR of 0.97717 µm corresponds to optimal process parameters, discharge current, T_{on}, T_{off}, and servo voltage at 90 A, 106 µs, 45 µs, and 50 V, respectively. The T_{on} was found to be the most significant parameter affecting the SR. The SEM-based image analysis suggested that Nimonic 90 alloys undergo fewer subsurface micro-cracks than steel. Singh Nain et al. [112] evaluated the SR of Nimonic 90 using a support vector machine, Gaussian process, and ANN modeling techniques. The authors carried out the WEDM experimental plan with Taguchi L

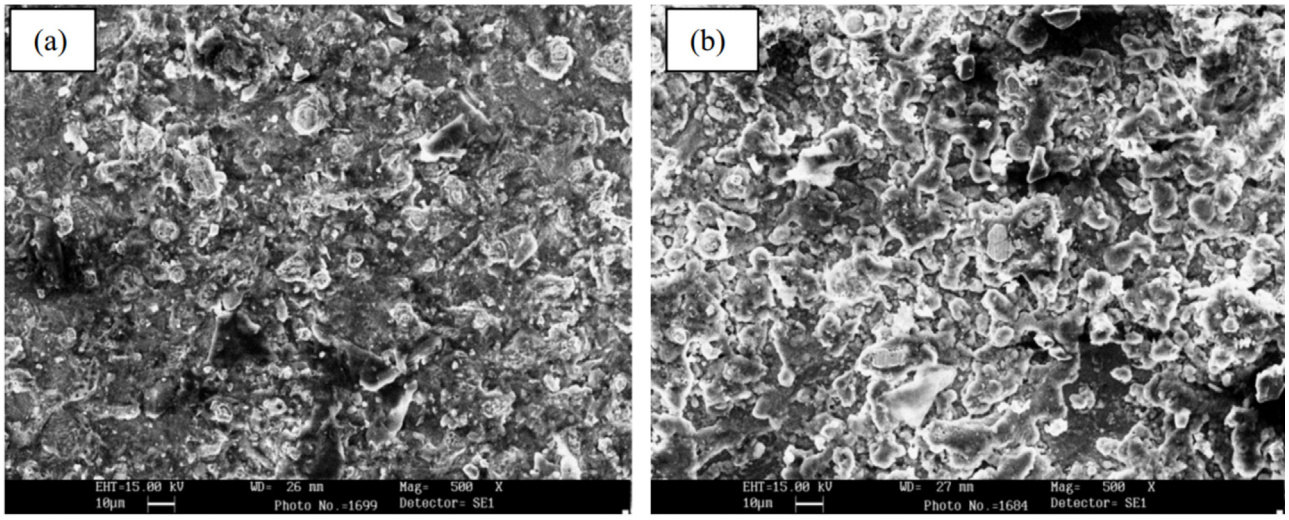

Fig. 21. Showing SEM images of Nimonic 90 surface during WEDM of Nimonic 90 at (a) low discharge energy, (b) high discharge energy [108].

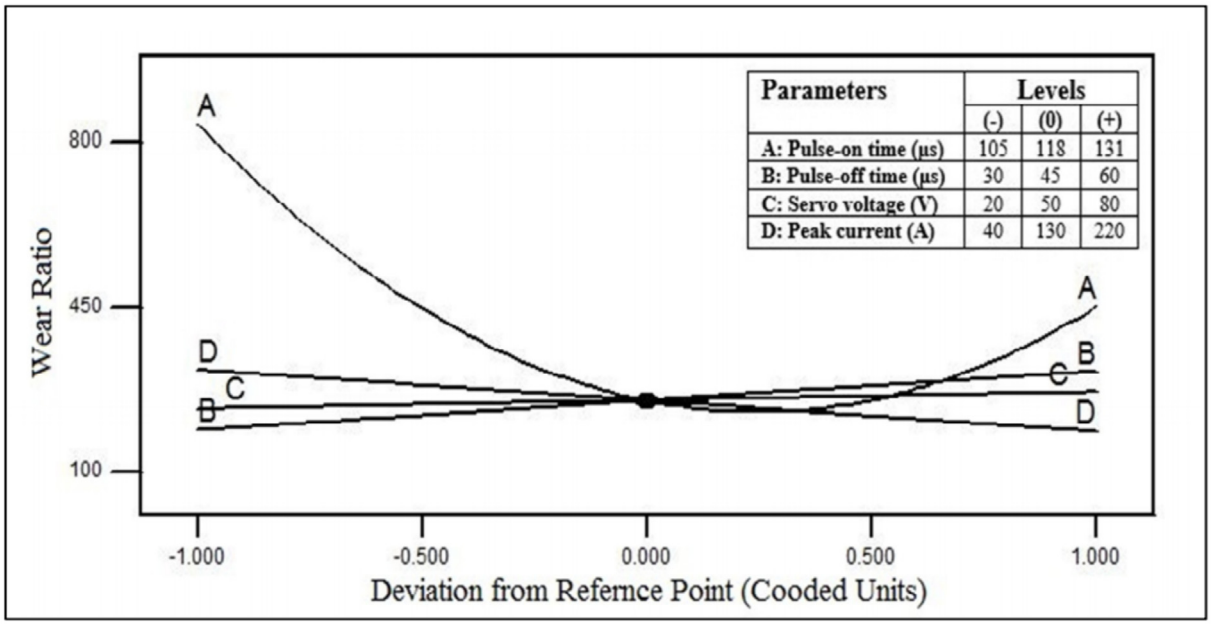

Fig. 22. Variation of T_{on}, T_{off}, servo voltage, and IP with wear ratio in WEDM of Nimonic C263 [110].

18 mixed-type array and measured the SR of the machined surface using a profilometer. The Gaussian model with the PUK kernel showed better results when compared with various other kernels used to predict the SR peculiarities. Singh et al. [113] stated that the kerf width was an essential parameter in deciding the dimensional accuracy of WEDM parts of Nimonic 75. The authors justified it further through ANOVA results that the kerf width and the MRR were most affected by the T_{off} followed by the T_{on}. The authors also identified minimum kerf width and maximum MRR corresponding to the optimum values of process parameters viz., IP, servo voltage, T_{off}, T_{on} at 200 A, 25 V, 14 µs, and 0.6 µs, respectively. In another study [114], the authors noted that the kerf width increased with the T_{on} and decreased with the T_{off}. Sonawane and Kulkarni [21] used the principal component analysis (PCA) integrated with the Taguchi method to optimize the responses viz., SR, overcut, and MRR in the WEDM of Nimonic 75. The authors recorded the optimum values of process parameters viz., T_{on}, T_{off}, servo voltage, IP, wire FR, and wire tension at 110 µs, 51 µs, 40 V, 230 A, 5 m/min, and 8 g, respectively. In addition, authors have also used ANOVA, which identified T_{on} as the most influencing factor, with a 52.89% contribution to responses.

Goswami and Kumar [115] conducted the grey rational analysis on the WEDM of Nimonic 80A and reported that the optimum values of the process parameters viz., T_{on}, T_{off}, IP, wire FR, wire tension, and servo voltage were

Fig. 23. Chip formation under conventional turning (CT) and UAT of Nimonic 90 superalloy under dry and wet conditions [136].

118 µs, 30 µs, 80 A, 6 m/min and 7 g, and 30 V respectively. The analysis showed that T_{on} and T_{off} were the most significant factors affecting the MRR with the contribution of 46% and 33%, respectively. On the other hand, the wire wear ratio was influenced by the interaction effect of parameters viz., $T_{on} \times T_{off,}$ and $T_{on} \times$ IP. The same authors in [116] predicted and optimized the wear ratio, SR, and MRR during the WEDM of Nimonic 80A. The results of the MOO showcased the optimum values of the process parameters viz., IP, wire offset, T_{on}, T_{off} on responses viz., SR, wear ratio and MRR as 60 A, 0.08 mm, 0.6 µs and 14 µs, respectively. The ANOVA results further revealed that the T_{on} was a significant factor influencing the MRR as well as SR with a confidence level of 52.31% and 74.69%, respectively. In contrast, the wear ratio of the wire was primarily affected by the wire offset with a 45.34% confidence level. Another group of researchers conducted MOO of the process parameters in WEDM of Nimonic C263. The authors observed that the 'technique for order preferences by similarity to an ideal solution' (TOPSIS) method outperformed other MOO techniques with optimum values of the SR and the MRR at 1.85 µm and 3.234 mm^3/min, respectively. Based on the above observations, the authors have put forth a strong case for using MOO-based techniques in the industry for enhanced productivity [117]. Reference [118], used a novel Bee Colony Cuckoo Search algorithm to optimize the process parameters viz., T_{on}, T_{off}, IP, and servo voltage of WEDM of Nimonic C263 and compared it with the results obtained from RSM. The comparative analysis revealed that the Bee Colony Cuckoo Search optimization method was superior to RSM. Chaudhary et al. [119] analyzed the process parameters of WEDM viz., IP, T_{off}, T_{on}, wire tension, and dielectric fluid on the responses viz., SR, machining time, MRR, kerf width, surface micro-hardness, and depth of micro-hardness using Entropy-TOPSIS and Pareto ANOVA techniques. It was concluded from the analysis that dielectric fluid (60% of demineralized water + 40% Ethelene glycol), IP 3 A, T_{off} 2 µs, wire tension 6 N, and T_{on} 15 µs were the optimum values of influencing parameter (in the order) for better machining performance. A similar result was seen during a MOO of the process parameters on the dimensional accuracy. The investigation revealed the order of significance of process parameters as follows, viz., T_{on} (20 µs), dielectric fluid (demineralized water (60%) + Ethylene Glycol (40%), IP (3 A), T_{off} (4 µs), and wire tension (18 N) respectively [120]. Sonawane and Kulkarni [121] converted the multi-objective problem into a single objective problem using PCA-based utility theory in the case of WEDM of Nimonic 75 superalloy. The results showed the optimum values of process parameters viz., T_{on}, T_{off}, discharge current, discharge voltage, wire FR, and wire tension at 114 µs, 51 µs, 200 A, 20 V, 5 m/min, and 2 g, respectively. Mouralova et al. [122] performed MOO of the WEDM for minimum SR, kerf width, and maximum CS. The authors obtained the optimum value of process

parameters viz., gap voltage, T_{on}, T_{off}, wire FR, and discharge current at 50 V, 6 µs, 30 µs, 10 m/min and 31.67 A, respectively. Further, the T_{on} and the discharge current were the most influencing factors on the responses.

Many researchers have worked on modeling and optimizing EDM/WEDM process parameters to raise productivity. Since non-conventional machining of Nimonic superalloys is a niche area and holds extensive scope for high-quality research, much research related to optimization studies on EDM/WEDM of Nimonic superalloys was reported in the previous year. A brief summary of the optimization work published in the year 2021–22 on non-conventional machining of the Nimonic superalloys is presented in Table 5.

3.3 Other types of non-conventional machining

Khanna et al. [28] conducted a UAT operation of Nimonic 90 superalloy at the optimal CS, FR, DOC, and frequency of 61.14 m/min, 0.11 mm/rev, 0.1 mm, and 20 kHz, respectively, and analyzed the response (SR). The statistical analysis showed that the FR affected the surface quality most. Further, the authors concluded that the UAT produced the microchipping effect that helped to reduce the SR. According to Airao et al. [135], the UAT operation of Nimonic 90 has seen a 6–15% reduction in power consumption and 70–80% reduction in SR due to the recurrent separation of tool and work to conventional turning. SR was found to increase with the increase in the values of the cutting parameter due to the rise in the tool-work contact ratio. The study was further continued with the use of coolant and reported in [136] that the use of coolant has reduced the cutting force and feed force by 9% and 17%, respectively, compared to conventional wet turning. The primary wear mechanisms observed in both the above studies by Airao et al. are chipping, abrasion, notch wear, and adhesion. Additionally, the authors found that using coolant has reduced the adhesion of BUE on the cutting edge and the chips produced were thinner, smoother, and shorter than conventional turning. The comparison of various types of chips made in UAT and conventional turning under dry and wet conditions are presented in Fig. 23. The same authors in [137] developed a FEM for tool wear prediction in hot UAT. The closeness of agreement between predicted and experimental values were reported as 2–25%. The main tool wear mechanisms observed were adhesion, abrasion, chipping, BUE and fracture. The hot UAT reduced the cutting and feed force by 5–25% and 14–36%, respectively, compared to traditional turning and UAT. At higher CS, catastrophic failure of the cutting tool was observed.

Singh and Singh [138] compared the conventional and ultrasonic-assisted EDM (UAEDM) of Nimonic 75 alloy based on MRR and SR. The experimental observations showed that UAEDM increased the MRR and SR by 53.57% and 18.47%, respectively. Further, surface morphology studies indicated that UAEDM has fewer surface irregularities, viz., crater, micro-pores and debris, than EDM surface. In addition, the Cu electrode resulted in more SR for both processes than the brass electrode. Singh and Sharma [139] conducted ultrasonic-assisted grinding studies on Nimonic 80A using green atomized cutting fluid to increase productivity. The proposed methodology significantly reduced the normal force, tangential and SR by 66.22%, 52.66% and 46.48%, respectively. Also, the proposed methodology provided better lubrication in the grinding zone by reducing the coefficient of friction by 30.42% compared to conventional grinding.

Unune et al. [140] conducted the abrasive mixed electro-discharge diamond grinding on Nimonic 80A and obtained the optimum values of the process parameters viz., powder concentration, wheel speed, T_{on} and current at 4 g/L, 1400 rpm, 26 µs, and 10 A, respectively. The authors noted that the MRR is directly proportional to the wheel speed. Conversely, the MRR was found to increase initially with the addition of powder in the dielectric but decreased later with further addition, which was attributed to the inter-electrode joining gap. The authors reported the order of significance of various process parameters as CS, current, and powder concentration, with their contribution to the responses being 52.23%, 14.45%, and 14.45%, respectively. In another study by Unune et al. [141], proposed a fuzzy logic-based model and reported that when wheel speed varied from 700 to 1300 rpm, the SR decreased by 5.96%, and the MRR increased by 83.89%. The authors also observed that adding abrasives from 0 to 8 g/L, reduced the SR by 17.10%.

Yadav and Yadava [142] proposed a new method of drilling a hole in Nimonic superalloy (AE 435 grade) using electro-discharge diamond drilling. The authors have developed a Taguchi-based second-order RSM and found it adequate, with a confidence level of 99%. On the other hand, the process parameters were optimized using a combination of Grey Relational Analysis and PCA. The study discovered that the linear effects of the process parameters are significant for all three responses, viz., MRR, SR, and average circularity. The same group of authors also has the credit for developing a new method for drilling a hole in Nimonic superalloy (AE 435 grade) using a self-designed and developed metal-bonded diamond abrasive tool set installed in ZNC 320 sinking EDM machine. The authors have observed that SR increased with the gap current, which was attributed to the increased spark energy, leading to increased heat energy and discharge power. In addition, it produced a crater on the machined surface, thereby deteriorating the surface. The authors also noted the improved surface finish due to an increase in the DF and the tool electrode rpm and credited it to the effective flushing and removal of re-casted thermal-infested layers by the tool [143].

Mishra et al. [144] employed the electrochemical milling operation for machining an 'L' shaped feature on Nimonic C263 superalloy and achieved a minimum SR of 0.07-0.08 µm by optimizing the process parameters viz., tool rotation with internal flushing, tool structure, and the number of outlets on the end face of the tool and mixed electrodes ($NaCl + NaNO_3$). Also, the influence of electrolyte flow patterns on profile milled was analyzed by simulating tool rotation in ANSYS. The same research group also conducted the micro electrochemical milling operation of Nimonic C263 and reported the optimal values of process parameters viz. voltage, DF, frequency, FR,

Table 5. Summary of research work reported on optimization studies related to EDM/WEDM of Nimonic superalloys.

Reference	Work/ electrode/ dielectric	Input parameter	Output parameter	The focus of the work	Remark/Discussion
[123]	Nimonic 75/ Cu and brass/spark erosion oil	TM, IP, V_g, T_{on}, T_{off}, Tool lift time (TLT)	MRR, TWR, SR	MOO during EDM	Optimum parameters using Taguchi based grey relational analysis are TM = Cu, IP = 12 A, $V_g = 500$ V, $T_{on} = 200$ µs, $T_{off} = 15$ µs, TLT = 2 s
[124]	Nimonic 75/Cu, brass	TM, T_{on}, T_{off}, TLT, V_g, gap current	MRR, TWR, SR	MOO during ultrasonic-assisted EDM	Optimal parameters from Taguchi- grey relational analysis: TM = Cu, $T_{on} = 200$ µs, $T_{off} = 15$ µs, TLT = 2 s, $V_g = 15$ V, gap current = 12 A
[125]	Nimonic 90/ Cu/kerosene (powder = Si)	Powder concentration, discharge current, spark on duration, spark off duration	SR, recast layer thickness	Experimental instigation of powder-mixed EDM	Powder concentration = 12 g/L, discharge current = 3 A, spark on duration = 35 µs, spark off duration = 49 µs
[126]	Nimonic 80A/ zinc-coated brass wire electrode	IP, T_{on}, T_{off}, FR	SR	Optimization during WEDM	From ANOVA, SR increases with a decrease in the T_{off}; SR is minimized by increasing the T_{on} and IP
[127]	Nimonic 80A/ Mo/de-ionized water	Duty factor (DF), V_g, FR	MRR, wire wear ratio, SR	Optimization during WEDM	Dominant factor is DF; increase in DF all output responses increase; optimum parameters are DF = 0.8771, $V_g = 17$ V and FR = 17 m/min
[128]	Nimonic C263 /Cu, W, and Cu-W/ kerosene	IP, Vg, T_{on}, DF, TM	SEC, machining noise, MRR, TWR, SR, radial over cut	Sustainable EDM to evaluate and optimize the responses	Optimal values from hybrid optimization; IP = 3 A, $V_g = 60$ V, $T_{on} = 100$ µs, DF = 85%, TM = Cu T_{on} has great influences on SEC; IP, and TM have a significant impact on noise, TWR, and MRR; IP is a dominant factor for SR
[129]	Nimonic 80A/ Cu/ kerosene	IP, T_{on}, T_{off}	SR and MRR	MOO during EDM of Nimonic 80A	Optimum RSM parameters; IP = 13.49 A, $T_{on} = 150$ µs, $T_{off} = 4$ µs; T_{on} shows the stronger effect on MRR followed by IP and T_{off}; T_{on} has both positive and negative impact on SR
[130]	Nimonic 80A/ brass wire/de-ionized water	IP, V_g, duty cycle, wire- speed	MRR and kerf width	Experimental investigation of WEDM of Nimonic 80A and MOO	RSM optimum WEDM parameters: IP = 57 A, $V_g = 90$ V, duty cycle = 75 µs, wire speed = 7 mm/min; IP shows high impact on MRR and kerf width

Table 5. (continued).

Reference	Work/ electrode/ dielectric	Input parameter	Output parameter	The focus of the work	Remark/Discussion
[131]	Nimonic 901/ Cu–W	T_{on}, IP, servo voltage, powder concentration	SR, TWR, MRR	Optimization of parameters of powder-mixed EDM	From statistical results optimum parameters were T_{on} = 20 µs, IP = 5 A, servo voltage = 5 V, powder concentration = 10 weight%
[132]	Nimonic 90 /Cu	T_{on}, T_{off}, IP, powder concentration	SR, TWR, MRR	Optimization of parameters of powder (µ-titanium carbide) - mixed EDM	Grey relational analysis based optimum parameters were T_{on} = 30 µs, T_{off} = 2 µs, IP = 20 A, powder concentration = 4 g/L
[133]	Nimonic C263/ Mo	T_{on}, T_{off}, IP, voltage	SR, MRR, cycle time	Optimization of the WEDM process	T_{on} and T_{off} most influencing parameters; optimum parameter for MRR were T_{on} = 30 µs, T_{off} = 8 µs, IP = 4 A, voltage = 80 V
[134]	Nimonic 80A/ CBN grinding wheel	Air pressure, DOC, rotational speed, vibration intensity, stand-off-distance	Normal force, tangential force, SR	MOO of parameters of ultrasonic-assisted grinding	Optimum parameters from the statistical analysis: air pressure = 4 bar, DOC = 49.10 µm, rotational speed = 2198.02 RPM, vibration intensity = 56.85%, stand-off-distance = 52.99 mm

DOC, and tool speed for responses viz., minimum SR, and overcut as 7.5 V, 40%, 50 kHz, 1.5 mm/min, 100 µm, and 750 rpm respectively [145]. Shamli et al. [146] stated that lower SR, circularity entry, and exit were achieved during the electrochemical micromachining using an electrolyte ($NaNO_3$ (5 g), NaCl (2.5 g)) than ($C_2H_6O_2$ (2.2 ml), NaBr (2.2 g), HF acid (3.2 ml)) electrolyte. Further, the authors revealed from ANOVA results that voltage was the most influencing factor.

Even laser drilling is the widely used non-conventional machining process to manufacture effusion cooling holes at acute angles on aerospace components made of superalloys. Ezhilarasan et al. [147] quantitatively analyzed the heat-affected zone, recast layer, and hole taper during the laser drilling of holes on Nimonic C263. The recast layer, heat-affected zone, and hole taper were found to be affected by pressure, power, and type of gas used for laser generation. Sibalija et al. [148] conducted laser cutting of Nimonic C263 and optimized the process parameters using ANN and particle swarm optimization techniques. The author concluded that the quality of the cut area, microstructure, and mechanical properties could be improved significantly by using the laser cutting method. Bagchi et al. [149] researched the abrasive jet machining of Nimonic superalloy and claimed that machining at a lower speed is better for getting a good surface finish (Fig. 24a). Further, the authors also claimed that low CS, accompanied by a high-pressure jet and low stand-off distance, improved MRR along with the surface finish (Fig. 24b). An experimental study by Madhavarao et al. [150] appraised the abrasive water jet machining of Nimonic C263 superalloy and reported that transverse speed was an important parameter affecting MRR, SR, and kerf taper. The authors observed that MRR increased with an increase in transverse speed and water jet pressure under ideal conditions. Conversely, SR increased with an increase in transverse speed up to 20 mm/min and then decreased, whereas the kerf taper decreased with an increase in water jet pressure up to 220 MPa and then increased.

3.4 Summary of the nonconventional machining process

Researchers have focused on MRR, SR, TWR, tool material and overcut during the EDM of Nimonic alloys. The tool material viz., Cu, W, Cu-W are commonly used for analyzing the EDM process. However, Cu is the most recommended one for EDM. The parameters viz., T_{on}, T_{off}, and IP are the most commonly considered inputs to EDM. Most research studies show IP is the most influencing parameter, followed by T_{on} and T_{off}. Researchers have shown great interest in comparing different tool materials, disk-type electrodes, powder-mixed EDM, modeling of EDM, etc. However, further studies need to address the recast layer formation, use of natural oil as dielectrics, debris removal from the electric gap, surface defects produced and dimensional accuracy of parts produced. The knowledge gap in powder mixed EDM of Nimonic alloys must be considered as a scope for future work.

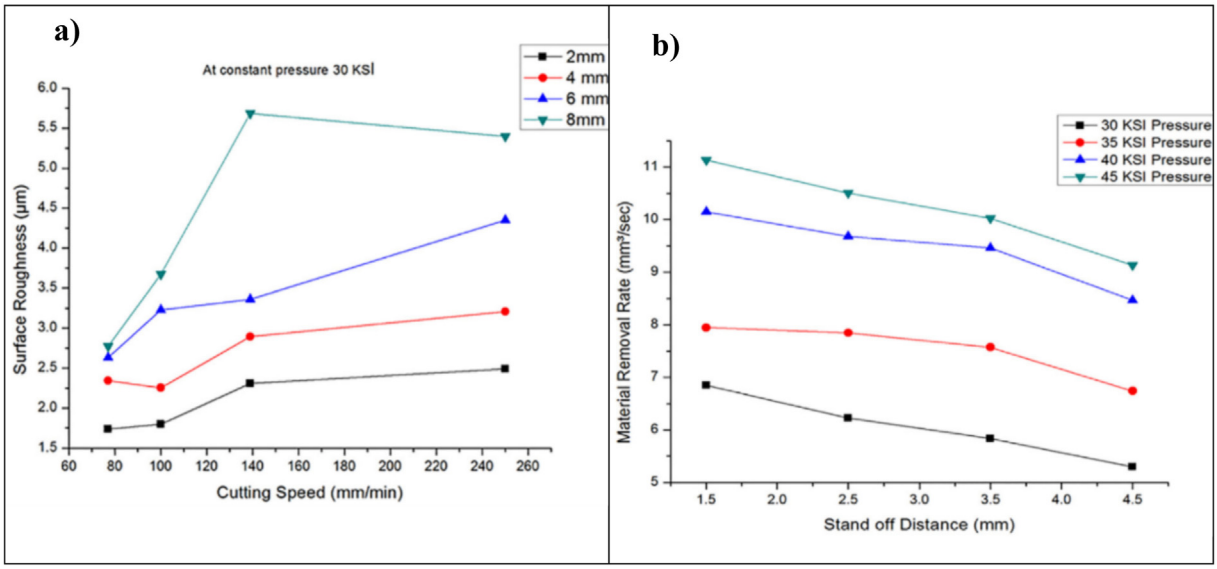

Fig. 24. Abrasive water jet parameter variation (a) SR with CS, (b) MRR with stand-off distance [149] (in Figure 24a) 2 mm, 4 mm, etc. indicating the distance in the DOC direction where SR is measured).

The WEDM-based studies mainly focused on the responses viz., SR, wire wear ratio, MRR, kerf width and overcut. T_{on}, T_{off}, discharge current, servo voltage, wire tension, wire feed and wire offset are some of the commonly considered input parameters. Research outcomes showed that T_{on} was the most significant factor influencing the responses. The different area of study in the case of WEDM includes optimization of process parameters, correlating the input and output parameters, trim and rough cutting and post-processing of the WEDM surface. The key research areas include selecting appropriate wire material, wire coating, selection of wire diameter, high-speed-cutting and study on mechanical and thermal characteristics of wire material.

There are diversified studies on non-conventional machining processes other than EDM/WEDM. UAT, UAT-based grinding, ultrasonic-assisted EDM, electro-discharge diamond grinding, electro-discharge diamond drilling, electrochemical machining, laser drilling, and abrasive water jet machining are some of the nonconventional studies researchers have investigated. Furthermore, studies are required, to address the cost-benefit analysis, material removal mechanism, mechanical and thermal characteristics, of the nonconventional machining as well as its productivity and reliability.

4 Trends and future directions

Now, all the manufacturing companies are attempting to compete in a global market that is becoming utmost demanding. New materials, manufacturing processes, and products have been researched and developed due to worldwide competition. The advanced design and manufacturing principles involved in manufacturing materials are essential to present advancement. Modern manufacturing processes have evolved due to the need to use new materials for various applications in industries and the need to control their dimensional accuracies. The ongoing implementation of an integrated environmental strategy inclusive of green manufacturing strategies aims to improve the ecological efficiency of processes, products, and services, thereby lowering the risks to workers and the environment to achieve the goal of sustainable production. In other words, sustainable production minimizes the reliance on natural resources, thereby significantly bringing down the negative environmental impact. Further, reduced pollution levels can be achieved by intelligently recycling trash or generating green products.

One such newly explored group of materials is superalloys in which Nimonic superalloys are most widely used, with more than fifty percent of usage seen in aircraft engines, especially in gas turbine components, due to their higher hardness, strength, and corrosion resistance compared to other materials. But, machining of Nimonic superalloys is challenging due to the high temperature resulting from the friction between the tool and the workpiece, especially during heavy load conditions, which increases the affinity of work material to weld along with tool material. In addition, maintaining the mechanical properties at high temperatures and poor thermal conductivity further leads to lower machinability. Thus, understanding the machinability of Nimonic superalloys and corresponding influencing parameters is essential.

Conventional machining processes like turning, milling, and many more are essential and unavoidable machining operations in various manufacturing sectors to machine parts suitable for assembly and achieve better surface quality. Even though many advanced machining techniques have emerged and become famous, conventional machining is still required to obtain precise components. The suitability of traditional machining techniques such as turning, milling, and drilling has been investigated by many researchers in the machining of Nimonic superalloys.

Machining studies regarding tool wear, SR, cutting force, use of coolant and lubrication, and modeling and optimization are conducted on turning and milling operations. Nevertheless, the studies on cutting force evaluation, development of cutting force model, cryogenic cooling, hybrid cooling system, and process parameter optimization are minimal. Dry machining could be considered the most sustainable option for machining Nimonic superalloys only if a suitable solution is found to overcome rapid temperature changes. Hence, a thorough investigation is required before the industry can use dry machining. Research studies about cutting tool coating have also been conducted to promote improved machinability, particularly cost savings. However, a cost-benefit analysis is required before such coating technology can be implemented. A good research approach would be to look at the life cycle of the coating material as well as the machining of the work material. Furthermore, future research into the tribological and thermo-mechanical effects of coating on machinability and environmental indices is worthwhile.

On the other hand, machining studies can be carried out simultaneously in dry and coolant/lubricant-assisted machining to achieve optimization of process parameters, followed by a relative comparison of the machined surfaces. In recent years researchers have also experimented with sustainable machining techniques (green machining techniques) by using air cooling, MQL, NMQL, cryogenics, and hybrid cooling (cryogenic + MQL) with a strong focus on reducing the non-biodegradable product waste, thereby having the minimal impact on the environment as well as on the worker's health. In that regard, further studies on optimizing the process parameters to increase the productivity of machining the Nimonic superalloys with sustainable techniques are the need of the hour.

It is also significant to investigate the drilling operation of Nimonic superalloys, as it differs significantly from the turning and milling operations. However, there is a scarcity of research that focuses on advancing the drilling studies on Nimonic superalloys. Also, drilling holes is a critical operation in aircraft engine components made of Nimonic superalloys [151]. Grinding is a standard industrial operation for creating final components with the proper form, size and accuracy. It accounts for 25% of all jobs as well as 43% of the total machines installed in manufacturing industries [152]. However, no studies have been reported in the literature about conventional grinding operations on Nimonic superalloys.

But, in the last decade, researchers have concluded that none of the conventional machining operations are favorable options while machining complicated target shapes on materials whose physical and mechanical properties vary beyond a specific limit. One such material is Nimonic superalloys. In that regard, researchers have explored various non-conventional methods, namely, EDM, WEDM and UAT, for machining Nimonic superalloys. EDM is a widespread technique among nonconventional machining processes to machine any conductive material, regardless of its mechanical properties. The shape of the EDMed surface is determined by electrical and non-electrical parameters, as well as the shape and accuracy of the tool geometry.

Furthermore, high wear resistance, good thermal and electrical conductivity and cost are the primary criteria for TM selection in EDM. The best TM is one that has a high electrical and thermal conductivity, as well as a high boiling and melting point. The researchers have used a variety of process parameters to investigate the EDM process, namely, T_{on}, T_{off}, TM, IP, V_g, DF, tool polarity, and tool feed. In contrast, the output machining characteristics include SR, MRR, electrode wear rate, and radial overcut. Optimization of the process parameters has resulted in the improved performance of EDM.

Conversely, the most challenging aspect of the EDM process is removing debris from the electrode gap. The debris formed by the melting of the workpiece metal gets accumulated in the electrode gap, making the machining process unstable and negatively affecting the MRR and surface integrity of the machined surface. Further research studies must overcome these problems by following some hybrid strategies. In addition, very few reported literatures are available on theoretical modeling and simulations of non-conventional machining of Nimonic superalloy using finite element analysis. A comprehensive simulation-based study is also required to understand the physics of EDM of Nimonic superalloys. Further research is needed as few works have been reported on powder-mixed EDM and micro EDM of Nimonic superalloys.

It is very well documented from the literature that WEDM is the widely used non-conventional machining technique for machining Nimonic superalloys. The research primarily focuses on modeling and optimizing process parameters (T_{on}, T_{off}, wire material, IP, V_g, cable tension, and many more) to achieve lower SR and wire wear rate along with higher MRR. Further research studies are required to get more clarity about minimizing surface defects, crater formation, SR, wire wear rate, and recast layer formation on the machined surface. Additionally, analysis of the wire temperature, wire deflection, changes in mechanical properties of the work material, machining using different wire diameters and wire coating, as well as cryogenic treatment of wire provide ample research opportunities. Further, developing cost-effective wire electrodes with high conductivity and high fracture toughness for high-speed-cutting will continue to be a focus of future research.

In EDM/WEDM of Nimonic superalloys, the best machining performance and reduced environmental impact can be achieved using dielectric fluids. But extreme caution should be exercised when choosing a dielectric fluid to ensure that the various types of metallic and gaseous waste emitted from hydrocarbon-based dielectrics are kept to a minimum. More research is needed in the areas of dry or near-dry machining and natural fluids as a dielectric medium. Some attempts have to be made to check the feasibility of using gaseous dielectrics such as air and oxygen in EDM.

Few studies have been reported on certain non-conventional machining techniques like abrasive mixed electro-discharge diamond grinding, electrical discharge diamond drilling, electrochemical milling, electrochemical micro-milling, laser cutting, and laser drilling. Further in-depth research needs to be conducted to study and enhance

Table 6. Showing composition and application of some unexplored materials under machining studies.

Material	Element (composition in weight%)	Applications
Nimonic 81	C (0.05), Si (0.5), Cu (0.2), Fe (1.0), Mn (0.5), Cr (30), Ti (1.8), Al (0.9), Co (2.0), Mo (0.3), B (0.003), Zr (0.06), S (0.015), Ni(B*)	Piston engine exhaust value, gas turbines, heat exchange plants
Nimonic 86	C (0.05), Cr (25.0), Mo (10.0), Mn (0.015), Ce (0.03), Ni (B)	Afterburner parts, gas turbine combustion chamber, hear treatment furnace component
Nimonic 105	C (0.17M*), Si (1.0M), Cu (0.2M), Fe (1.0M), Mn (1.0M), Cr (14.0–15.7), Ti (0.9–1.5), Al (4.5–4.9), Co (18.0–22.0), Mo (4.5–5.5), B (0.003–0.010), Zr (0.15M), S (0.010M), Pb (0.0015M), Ni (B)	Bolts and fasteners, turbine blades, discs, forgings, ring sections
Nimonic 115	C (0.12–0.2), Si (1.0M), Cu (0.2M), Fe (1.0M), Mn (1.0M), Cr (14.0–16.0), Ti (3.5–4.5), Al (4.5–5.5), Co (13.0–15.5), Mo (3.0–5.0), B (0.01–0.025), Zr (0.15M), S (0.015M), Pb (0.0015M), Ni (B)	Turbine blades for gas engine
Nimonic 901	Ni (42.5), Cr (12.5), Mo (5.75), Ti (2.9), Co (1.0M), Cu (0.5M), Mn (0.5M), Si (0.4M), Al (0.35M), C (0.1M), S (0.03M), Fe (B)	Gas turbine shafts, discs, rings, casings and seals with a maximum service temperature of 600 °C
Nimonic PE11	Ni (37.0–41.0), Fe (B), Cr (17.0–19.0), Mo (4.75–5.75), Ti (2.2–2.5), Al (0.7–1.0), C (0.03–0.08), Si (0.5M), Cu (0.5M), Mn (0.2M), Co (1.0M), B (0.001M), Zr (0.02–0.05), S (0.015M)	Components of gas turbines
Nimonic PE16	C (0.04–0.08), Si (0.5M), Mn (0.2M), S (0.015M), Ag (0.0005M), Al (1.1–1.3), B (0.005M), Bi (0.001M), Co (2.0M), Cr (15.5–17.5), Cu (0.5M), Mo (2.8–3.8), Ni+Co (42.0–45.0), Pb (0.0015M), Zr (0.02–0.04), Fe (B)	Missile hot components, gas turbine flame tubes, superheater tubing, nuclear reactor parts and aircraft ducting systems
Nimonic PK33	C (0.07M), Si (0.5M), Cu (0.2M), Fe (1.0M), Mn (0.5M), Cr (16.0–20.0), Ti (1.5–3.0), Al (1.7–2.5), Co (12.0–16.0), Mo (5.0–9.0), B (0.005M), Zr (0.06M), S (0.015M), Ni (B)	Combustion chambers, jet pipes and reheat systems for high-performance gas turbine engines

*B = Balance, M = Maximum.

the machinability of Nimonic superalloys to a larger extent. Additionally, researchers have reported that UAT is beneficial for the machining of Nimonic superalloy compared to conventional turning. Still, there is no reported evidence to justify the cost-benefit for the same.

Surface defects are one of the major problems in any machining operation, and it is no different in the machining of Nimonic superalloys, wherein various types of surface defects observed include surface cavities, cracking, carbide particles, and surface plucking. The ways to mitigate the surface defects involve either an appropriate selection of machining parameters and tool conditions or performing the finishing operations viz., grinding, lapping, and many more on the machined surface under the worst condition. On the other hand, SR, which is closely associated with the work material's thermal and mechanical deformation, poses another major problem during the machining of Nimonic superalloys. Some attempts have also been made to reduce SR using cryogenic cooling systems. Still, certain sections of the research community have raised concerns about the precooling of work material, resulting in increased cutting force required for machining operations leading to increasing tool wear. Also, the issue of the generation of compressive residual stress during cryogenic-assisted machining needs to be resolved with further research. Further, very few studies have been reported on the residual stress evaluation, chip morphology, work hardening, and formation of the white layer during the turning and milling operations on Nimonic superalloys.

Nowadays, industries are moving towards implementing the Industry 4.0 concept with the following automation. Image processing, machine learning, deep learning and cloud computing are some emerging technologies that help automate processes. Also, non-contact measuring the SR and TWR using a machine vision system is gaining more importance than the manual measurement system. However, no work has been reported using the above methods in the case of Nimonic machining presents a viable research gap.

Over the last few decades, tool condition monitoring has received much attention from academia, industry, and the research community as it decides the stability of the machining process, quality of machined surface and economics of machining. Tool condition monitoring involves measuring the tool wear land directly or indirectly. In the direct method, tool wear land is measured using microscopic devices, whereas, in the indirect method, signal processing (vibration, acoustic, current signals) and image

processing methods (images of wear land or machined surfaces) are used. Due to the rapid advances in indirect sensory technology, it is easier to process than a direct measurement. At the same time, indirect measurement has recently received much more attention with a continuous decrease in cost. However, no work has been reported on indirect tool wear monitoring methods in the Nimonic superalloy case. In addition, very little research has been reported on analyzing the status of different tool wear, tool wear mechanisms, and evaluation of nose wear and crater wear.

It is well understood that a workpiece machining characteristics are primarily determined by its composition, microstructure, and thermo-mechanical properties. As a result, assessing the machinability of other grades with significant engineering applications is crucial. Nimonic 81, Nimonic 86, Nimonic 105, Nimonic 115, Nimonic 901, Nimonic PE11, Nimonic PE16 and Nimonic PK33 are some of the Nimonic superalloys reported by the special metal corporation [31], but their machinability is unidentified. Table 6 shows the chemical composition and application of some unexplored Nimonic alloys under machining studies, mainly used in gas turbine applications.

5 Conclusion

Despite being difficult to cut material due to its low thermal conductivity and ability to retain hardness and strength even at high temperatures, Nimonic superalloys have found their applications in key sectors where lies the nation's economy. The paper provides a focused as well as an in-depth review of the current status of the conventional and nonconventional machining studies, along with the machining mechanisms related to the Nimonic superalloys. Following are some of the noteworthy conclusions summarised below:

- Nimonic 75, Nimonic 80A, Nimonic 90, and Nimonic C263 are the Nimonic superalloys that are commercially used and commonly available for machining studies.
- Turning and EDM/WEDM are the most widely used operations in conventional and nonconventional machining of Nimonic alloys.
- In the conventional machining processes, regular tool wear is a major problem leading to loss of productivity despite processes being much easier to conduct and less costly while machining simple parts. However, the authors have made the following key observations from the in-depth review of all the relevant articles. Firstly, the PVD-coated carbide insert with either MQL or cryogenic-based coolant is best suited for machining the Nimonic alloy. Secondly, the selection and optimization of the machining conditions play a major role in conventional machining. Third, productivity can be improved by carrying out machining at relatively high speed and medium values for FR and DOC. The authors have identified only a few studies on milling and drilling, whereas no reported studies on the grinding operation of Nimonic superalloys have come to the authors' knowledge.
- In non-conventional machining, most of the research works report the optimization of the process parameters and the responses and the discussions related to the significance of each parameter.
- Pulse duration and IP are identified as the most significant parameters that influence the responses in the EDM of Nimonic superalloys.
- Only a few studies reported on abrasive jet machining, laser cutting, and hybrid studies, viz., electrochemical milling, electrical discharge-based grinding and drilling, and UAT of Nimonic superalloys. Research works on these non-conventional machining of Nimonic superalloys are expected in the near future.</LIST>

Declaration of Competing Interest

The authors declare that they have no known competing financial interests or personal relationships that could have appeared to influence the work reported in this paper.

Symbols and abbreviation

T_{off}	Pulse off time
T_{on}	Pulse on time
V_g	Gap voltage
ANOVA	Analysis of variance
ANN	Artificial neural network
BUE	Built-up edge
CBN	Cubic boron nitride
CS	Cutting speed
CVD	Chemical vapor deposition
DOC	Depth of cut
DF	Duty factor
EDM	Electrical discharge machining
FCC	Face centered cube
FR	Feed rate
IP	Peak current
LCO_2	Liquid carbon dioxide
LN_2	Liquid nitrogen
MRR	Material removal rate
MQL	Minimum quantity lubrication
MOO	Multi-objective optimization
NMQL	Nanoparticle mixed minimum quantity lubrication
PVD	Physical vapor deposition
PCA	Principal component analysis
RSM	Response surface methodology
SEM	Scanning electron microscope
SEC	Specific energy consumption
SR	Surface roughness
TLT	Tool lift time
TM	Tool material
TOPSIS	Technique for order preferences by similarity to an ideal solution
TWR	Tool wear rate
UAT	Ultrasonic assisted turning
WEDM	Wire-cut electrical discharge machining

References

1. K. Nimel Sworna Ross et al., Investigation of surface modification and tool wear on milling Nimonic 80A under hybrid lubrication, Tribol. Int. (2020) 1–12
2. S. Akincioglu, H. Gokkaya, I. Uygur, The effects of cryogenic-treated carbide tools on tool wear and surface roughness of turning of Hastelloy C22 based on Taguchi method, Int. J. Adv. Manuf. Technol. **82** (2016) 303–314
3. N. Khanna, P. Shah, C. Agrawal, F. Pusavec, H. Hegab, Inconel 718 machining performance evaluation using indigenously developed hybrid machining facilities: experimental investigation and sustainability assessment, Int. J. Adv. Manuf. Technol. **106** (2020) 4987–4999
4. A. Suarez, F. Veiga, L.N.L. de Lacalle, R. Polvorosa, A. Wretland, An investigation of cutting forces and tool wear in turning of Haynes 282, J. Manuf. Process. **37** (2019) 529–540
5. A. Kumar, K. Maity, Modeling of machining parameters affecting flank wear and surface roughness in hot turning of Monel-400 using response surface methodology (RSM), Measurement **137** (2019) 375–381
6. K.V. Ramanan, S. Ramesh Babu, M. Jebaraj, K. Nimel Sworna Ross, Face turning of Incoloy 800 under MQL and nano-MQL environments, Mater. Manuf. Process. **36** (2021) 1769–1780
7. C.V. Yildirim, T. Kivak, F. Erzincanli, Influence of different cooling methods on tool life, wear mechanisms and surface roughness in the milling of Nickel-based Waspaloy with WC tools, Arab. J. Sci. Eng. **44** (2019) 7979–7995
8. E.P. Bonhin et al., Effect of machining parameters on turning of VAT32 ® superalloy with ceramic tool, Mater. Manuf. Process. (2019) 1–7
9. S. Singh, Superalloys Report, Tech. Rep. (2016) 1–40
10. W. Chunchun, J. Keyu, C. Gang, Hot compression deformation characteristics of Nimonic alloy as-forged, J. Phys. Conf. Ser. **1676** (2020) 1–7
11. N. Prasad Eswara, R.J. Wanhill, Aerospace Materials and Material Technologies 1 (2017)
12. A. Behera, Advanced Materials (Springer, Cham, 2022)
13. S. Miller, Advanced materials mean advanced engines, Interdiscip. Sci. Rev. **21** (1996) 117–129
14. R. M'Saoubi et al., High performance cutting of advanced aerospace alloys and composite materials, CIRP Ann. Manuf. Technol. **64** (2015) 557–580
15. O. Ozgun, H.O. Gulsoy, F. Findik, R. Yilmaz, Microstructure and mechanical properties of injection moulded Nimonic-90 superalloy parts, Powder Metall. **55** (2012) 405–414
16. S. Metal Corporation, NIMONIC alloy 75, SMC-058 (2004), pp. 1–4
17. G. Khajuria, M.F. Wani, High-temperature friction and wear studies of Nimonic 80A and Nimonic 90 against Nimonic 75 under dry sliding conditions, Tribol. Lett. **65** (2017) 1–26
18. S. metals Corporation, Nimonic 263, SMC-054 (2004), pp. 1–12
19. R. Choudhary, V. Kumar, Y. Batra, A. Singh, Performance and surface integrity of Nimonic75 alloy machined by electrical discharge machining, Mater. Today Proc. **2** (2015) 3481–3490
20. H. Bisaria, P. Shandilya, Experimental investigation on wire electric discharge machining (WEDM) of Nimonic C-263 superalloy, Mater. Manuf. Process. **34** (2019) 83–92
21. S.A. Sonawane, M.L. Kulkarni, Optimization of machining parameters of WEDM for Nimonic-75 alloy using principal component analysis integrated with Taguchi method, J. King Saud Univ. – Eng. Sci. **30** (2018) 250–258
22. P. Pant, P.S. Bharti, Electrical Discharge Machining (EDM) of nickel-based nimonic alloys: a review, Mater. Today Proc. **25** (2019) 765–772
23. M. Singh, S. Singh, Multi-objective optimization of electrical discharge machining of Nimonic 75 using teaching learning based optimization (TLBO) algorithm, Mater. Today Proc. **24** (2020) 576–584
24. M.E. Korkmaz, N. Yasar, M. Günay, Numerical and experimental investigation of cutting forces in turning of Nimonic 80A superalloy, Int. J. Eng. Sci. Technol. **23** (2020) 664–673
25. M.E. Korkmaz, P. Verleysen, M. Günay, Identification of constitutive model parameters for nimonic 80A superalloy, Trans. Indian Inst. Met. **71** (2018) 2945–2952
26. S.W. Kang, S.J. Heo, J.H. Yoo, J.H. Kang, Hardness prediction of a cold rolled nimonic 80A exhaust valve spindle, J. Achiev. Mater. Manuf. Eng. **94** (2019) 13–21
27. K. Venkatesan, S. Devendiran, D. Sachin, J. Swaraj, Investigation of machinability characteristics and comparative analysis under different machining conditions for sustainable manufacturing, Meas. J. Int. Meas. Confed. **154** (2020) 1–20
28. N. Khanna et al., Optimization of power consumption associated with surface roughness in ultrasonic assisted turning of Nimonic-90 using hybrid particle swarm-simplex method, Materials (Basel). **12** (2019) 1–20
29. C. Ezilarasan, V.S. Senthil Kumar, A. Velayudham, An experimental analysis and measurement of process performances in machining of nimonic C-263 super alloy, Measurement **46** (2013) 185–199
30. J. Jadav, K.R.V. Rajulapati, N. Eswaraprasad, and K. Bhanu Sankara Rao, Effect of temperature on tensile flow behaviour of Nimonic C-263 alloy, Mater. Today Proc. **5** (2018) 5475–5480
31. S. Metal Corporation, Nimonic, Special metals corporation, www.specialmetals.com
32. P.S. Jadhav, C.P. Mohanty, S.S. Shirguppikar, Cryogenic treatment of Nimonic alloy-hard turning : state -of- the-art, challenges and future directions, Mater. Today Proc. **18** (2019) 4120–4132
33. D.G. Thakur, B. Ramamoorthy, L. Vijayaraghavan, Study on the machinability characteristics of superalloy Inconel 718 during high speed turning, Mater. Des. **30** (2009) 1718–1725
34. S.H. Musavi, B. Davoodi, S.A. Niknam, Effects of reinforced nanoparticles with surfactant on surface quality and chip formation morphology in MQL-turning of superalloys, J. Manuf. Process. **40** (2019) 128–139
35. Chetan, S. Ghosh, P.V. Rao, Performance evaluation of deep cryogenic processed carbide inserts during dry turning of Nimonic 90 aerospace grade alloy, Tribol. Int. **115** (2017) 397–408
36. Chetan, B.C. Behera, S. Ghosh, P.V. Rao, Wear behavior of PVD TiN coated carbide inserts during machining of Nimonic 90 and Ti6Al4V superalloys under dry and MQL conditions, Ceram. Int. **42** (2016) 14873–14885
37. A. Bordin, S. Bruschi, A. Ghiotti, P.F. Bariani, Analysis of tool wear in cryogenic machining of additive manufactured Ti6Al4V alloy, Wear **328–329** (2015) 89–99

38. A. Thakur, S. Gangopadhyay, Influence of tribological properties on the performance of uncoated, CVD and PVD coated tools in machining of Incoloy 825, Tribol. Int. **102** (2016) 198–212
39. C. Ezilarasan, V.S. Senthil Kumar, A. Velayudham, Effect of machining parameters on surface integrity in machining Nimonic C-263 super alloy using whisker-reinforced ceramic insert, J. Mater. Eng. Perform. **22** (2013) 1619–1628
40. G.M. Krolczyk et al., Ecological trends in machining as a key factor in sustainable production – a review, J. Clean. Prod. **218** (2019) 601–615
41. R.P. Gama, M.V. Ribeiro, Effects of cutting fluid application in the performance of the nimomic 80A turning, Key Eng. Mater. **656–657** (2015) 243–250
42. K. Zhuang, X. Zhang, D. Zhu, H. Ding, Employing preheating- and cooling-assisted technologies in machining of Inconel 718 with ceramic cutting tools: towards reducing tool wear and improving surface integrity, Int. J. Adv. Manuf. Technol. **80** (2015) 1815–1822
43. T. Patel et al., Machinability analysis of nickel-based superalloy Nimonic 90: a comparison between wet and LCO2 as a cryogenic coolant, Int. J. Adv. Manuf. Technol. **113** (2021) 3613–3628
44. A. Singh, S. Ghosh, S. Aravindan, Flank wear and rake wear studies for arc enhanced HiPIMS coated AlTiN tools during high speed machining of nickel-based superalloy, Surf. Coatings Technol. **381** (2020) 1–15
45. A. Thakur, S. Gangopadhyay, A.M. Mohanty, K. Maity, Experimental assessment on performance of TiN/TiCN/Al2 O3/ZrCN coated tool during dry machining of Nimonic C-263, Int. J. Mach. Mach. Mater. **18** (2016) 452–465
46. V.K. Velmurugan, K. Venkateshan, S. Devendiran, A.T. Mathew, Dry machining of Nimonic 263 alloy using PVD and CVD inserts, Innov. Des. Anal. Dev. Pract. Aerosp. Automot. Eng. Lect. Notes Mech. Eng. (2019) 179–198
47. C. Ezilarasan, V.S. Senthil Kumar, A. Velayudham, K. Palanikumar, Assessment of factors influencing tool wear on the machining of Nimonic C-263 alloy with PVD coated carbide inserts, Adv. Mater. Res. **291–294** (2011) 794–799
48. Chetan, S. Ghosh, P.V. Rao, Comparison between sustainable cryogenic techniques and nano-MQL cooling mode in turning of nickel-based alloy, J. Clean. Prod. **231** (2019) 1036–1049
49. F.J. Xavier, B. Ravi, D. Jayabalakrishnan, C. Ezilarasan, V. Jayaseelan, G. Elias, Experimental study on surface roughness and flank wear in turning of Nimonic C263 under dry cutting conditions, J. Nanomater. 2021 (**2021**) 1–11
50. M. Dhananchezian, K. Rajkumar, Comparative study of cutting insert wear and roughness parameter (Ra) while turning Nimonic 90 and Hastelloy C-276 by coated carbide inserts, Mater. Today Proc. **22** (2020) 1409–1416
51. M. Singh, S. Gangopadhyay, Effect of cutting parameter and cutting environment on surface integrity during machining of Nimonic C-263a Ni based superalloy, 2017 Int. Conf. Adv. Mech. Ind. Autom. Manag. Syst. (2017), pp. 231–238
52. V. Chavan, S. Kadam, M. Sadaiah, Performance of alumina-based ceramic inserts in high-speed machining of nimonic 80A, Mater. Manuf. Process. **34** (2019) 8–17
53. K. Venkatesan, A. Thakur, A comparative study on machinability characteristics in dry machining of Nimonic 263 alloy using coated carbide inserts, Mater. Today Proc. **5** (2018) 12443–12452
54. M. Gunay, M.E. Korkmaz, N. Yasar, Performance analysis of coated carbide tool in turning of Nimonic 80A superalloy under different cutting environments, J. Manuf. Process. **56** (2020) 678–687
55. K. Venkatesan, S. Devendiran, A. Thakur, V. Ashish Chauhan, P.V. Pavan Kalyan, Study on influence of machinability characteristics in machining of nimonic 90A alloy using copper oxide nanofluid in MQL mode, Int. J. Mech. Eng. Technol. **9** (2018) 978–986
56. Chetan, S. Ghosh, P.V. Rao, Specific cutting energy modeling for turning nickel-based Nimonic 90 alloy under MQL condition, Int. J. Mech. Sci. **146–147** (2018) 25–38
57. M.E. Korkmaz, M.K. Gupta, M. Boy, N. Yasar, G.M. Krolczyk, M. Günay, Influence of duplex jets MQL and nano-MQL cooling system on machining performance of Nimonic 80A, J. Manuf. Process. **69** (2021) 112–124
58. V. Kannan, Experimental study of an eco-friendly turning process of nimonic 75 combining minimum quantity lubrication and hexagonal boron nitride-enhanced neem and jatropha oil nanofluids, J. Inst. Eng. Ser. C **103** (2022) 785–812
59. P.S. Jadhav, C.P. Mohanty, T.K. Hotta, M. Gupta, An optimal approach for improving the machinability of Nimonic C-263 superalloy during cryogenic assisted turning, J. Manuf. Process. **58** (2020) 693–705
60. S. Senthil Kumar, M.P. Sudeshkumar, C. Ezilarasan, S. Palani, J. Veerasundaram, Modelling and simulation of machining attributes in dry turning of aircraft materials Nimonic C263 using CBN, Manufactur. Rev. **8** (2021) 30
61. S.C. Bose, C.S.P. Rao, Modelling and prediction of surface roughness, cutting force and temperature while machining Nimonic-75 and Nicrofer C-263 super alloys using artificial neural network, Int. J. Mech. Eng. Technol. **3** (2012) 599–613
62. C. Ezilarasan, V.S. Senthil Kumar, A. Velayudham, K. Palanikumar, Modeling and analysis of surface roughness on machining of Nimonic C-263 alloy by PVD coated carbide insert, Trans. Nonferrous Met. Soc. China 21 (2011) 1986–1994
63. C. Ezilarasan, V.S. Senthil Kumar, A. Velayudham, Theoretical predictions and experimental validations on machining the Nimonic C-263 super alloy, Simul. Model. Pract. Theory **40** (2014) 192–207
64. M. Krishna et al., Application of MOORA & COPRAS integrated with entropy method for multi-criteria decision making in dry turning process of Nimonic C263, Manuf. Rev. **9** (2022) 1–10
65. S. Lakshmana Kumar, M. Thenmozhi, R.M. Bommi, C. Ezilarasan, V. Sivaraman, S. Palani, Surface roughness evaluation in turning of Nimonic C263 super alloy using 2D DWT histogram equalization, J. Nanomater. **2022** (2022) 1–11
66. R.M. Bommi, C. Ezilarasan, M.P. Sudeshkumar, T. Vinoth, Estimation of flank wear in turning of nimonic C263 super alloy based on novel MSER algorithm and deep patten network, Russ. J. Nondestruct. Test. **58** (2022) 140–156
67. A.H. Elsheikh et al., A comprehensive review on residual stresses in turning, Adv. Manuf. **10** (2022) 287–312
68. S. Gowthaman, T. Jagadeesha, Neetu, Effect of severe plastic deformation through machining on the microstructure and corrosion behavior of end milled nimonic 263 alloy, Mater. Lett. **275** (2020) 1–5

69. S. Gowthaman, T. Jagadeesha, Experimental investigations on the effect of severe plastic deformation through end milling on X-Ray peak broadening and microcrystalline characteristics of Nimonic 263, Trans. Indian Inst. Met. **73** (2020) 1215–1226
70. S. Gowthaman, T. Jagadeesha, Influence of radial rake angle and cutting conditions on friction during end milling of Nimonic 263, Int. J. Adv. Manuf. Technol. **109** (2020) 247–260
71. S. Gowthaman, T. Jagadeesha, Experimental study on the surface and interface phenomenon changes by means of contact angle measurement on slot milled nimonic 263 alloy, Mater. Lett. **285** (2021)
72. C. Ezilarasan, J. Francis Xavier, P. Shanmugaselvam, P. Balu, M. Nagaraj, Experimental analysis on machining attributes in milling of nickel based super alloy Nimonic C-263, Adv. Mater. Process. Technol. (2021) 1–13
73. S. Gowthaman, T. Jagadeesha, Effect of severe plastic deformation during slot milling on wear resistance and surface characteristics of nimonic 263 alloy, Eng. Res. Express **3** (2021)
74. S. Gowthaman, T. Jagadeesha, Influence of cutting environment and machining parameters on the cutting force and surface roughness of slot milled Nimonic 263 alloy, Multiscale Multidiscip. Model. Exp. Des. (2021)
75. S. Gowthaman, T. Jagadeesha, Experimental investigation on friction formation during slot milling of Nimonic263, Mater. Manuf. Process. **36** (2021) 1403–1413
76. S. Gowthaman, T. Jagadeesha, Comparative study on the critical effect of radial rake angle and machining parameters on the formation of vibration amplitude during end milling of Nimonic 263, Sadhana – Acad. Proc. Eng. Sci. **46** (2021) 1–13
77. S. Gowthaman, T. Jagadeesha, V. Dhinakaran, Influence of machining behavior on severe deformation and corrosion resistance of end milled Nimonic 263 alloy, Sadhana – Acad. Proc. Eng. Sci. **46** (2021) 1–9
78. S. Shekhar, S. Gowthaman, T. Jagadeesha, Effect of MQL, wet and dry lubrication on functional behavior of end milled nimonic-263, IOP Conf. Ser. Mater. Sci. Eng. **912** (2020) 1–12
79. K. Nimel Sworna Ross, G. Manimaran, Effect of cryogenic coolant on machinability of difficult-to-machine Ni–Cr alloy using PVD-TiAlN coated WC tool, J. Br. Soc. Mech. Sci. Eng. **41** (2019) 1–14
80. B. Podder, S. Paul, Improvement of machinability in end milling of Nimonic C-263 by application of high pressure coolant, Int. J. Mach. Mach. Mater. **11** (2012) 418–433
81. K.N.S. Ross, G. Manimaran, Machining investigation of Nimonic-80A superalloy under cryogenic CO2 as coolant using PVD-TiAlN/TiN coated tool at 45° nozzle angle, Arab. J. Sci. Eng. **45** (2020) 9267–9281
82. N.S. Ross, M. Mia, S. Anwar, M.G.M. Saleh, S. Ahmad, A hybrid approach of cooling lubrication for sustainable and optimized machining of Ni-based industrial alloy, J. Clean. Prod. **321** (2021)
83. N.S. Ross et al., Impact of hybrid cooling approach on milling and surface morphological characteristics of Nimonic 80A alloy, J. Manuf. Process. **73** (2022) 428–439
84. H. Hassanpour, M.H. Sadeghi, S. Shajari, M. Emami, Empirical modeling and analysis of surface roughness in milling process of Nickel-based super alloy Nimonic 115 through response surface methodology, Adv. Mater. Res. **325** (2011) 430–435
85. P. Giridhar Reddy, S. Gowthaman, T. Jagadeesha, Optimization of cutting parameters based on surface roughness and cutting force during end milling of nimonic C-263 alloy, 3rd Int. Conf. Adv. Mech. Eng. **912** (2020) 1–9
86. S. Gowthaman, T. Jagadeesha, Experimental investigation of surface morphological changes during end milling of nimonic 263, Surf. Topogr. Metrol. Prop. **7** (2019)
87. C. Ezilarasan, M.S. Nagaraj, A.J.P. Kumar, A. Velayudham, R. Betala, Experimental analysis of process parameters in drilling nimonic C263 alloy under nano fluid mixed MQL environment, Manuf. Rev. **8** (2021) 1–20
88. M. Nagaraj, A.J.P. Kumar, C. Ezilarasan, R. Betala, Finite element modeling in drilling of Nimonic C-263 alloy using deform-3D, Comput. Model. Eng. Sci. **118** (2019) 679–692
89. S. Lakshmana Kumar, V. Jacintha, A. Mahendran, R.M. Bommi, M. Nagaraj, U. Kandasamy, A machine learning approach to optimize, model, and predict the machining factors in dry drilling of nimonic C263, Adv. Mater. Sci. Eng. (2022)
90. A. Kale, N. Khanna, A review on cryogenic machining of super alloys used in aerospace industry, Proc. Manuf. **7** (2017) 191–197
91. N. Mohd Abbas, D.G. Solomon, M. Fuad Bahari, A review on current research trends in electrical discharge machining (EDM), Int. J. Mach. Tools Manuf. **47** (2007) 1214–1228
92. T. Muthuramalingam, B. Mohan, A review on influence of electrical process parameters in EDM process, Arch. Civ. Mech. Eng. **15** (2015) 87–94
93. D. Sahu, S.K. Sahu, T. Jadam, S. Datta, Electro-discharge machining performance of Nimonic 80A: an experimental observation, Arab. J. Sci. Eng. **44** (2019) 10155–10167
94. U.A. Kumar, G. Saidulu, P. Laxminaryana, Experimental investigation of process parameters for machining of nimonic alloy 75 using wire-cut EDM, Mater. Today Proc. **27** (2020) 1362–1368
95. R.K. Shastri, C.P. Mohanty, Sustainable electrical discharge machining of Nimonic C263 superalloy, Arab. J. Sci. Eng. (2021)
96. R.K. Shastri, C.P. Mohanty, Machinability investigation on Nimonic C263 alloy in electric discharge machine, Mater. Today Proc. **26** (2019) 529–533
97. S. Ramesh, P. Jenarthanan, Investigating the performance of powder mixed electric discharge machining of Nimonic 75 by using different tool materials, World J. Eng. (2017)
98. R.K. Shastri, C.P. Mohanty, A cost effective approach to explore the electrical discharge machined surface characteristics of Nimonic C263 superalloy, J. Mater. Eng. Perform. **31** (2022) 9748–9767
99. J. Vivek, P.V.A. Kumar, K.A.S. Lewise, V. Velmurugan, Improvement in the graphite electrode wear characteristic of electrical discharge machined Nimonic 90 through plasma nitriding, laser hardening and duplex process, Sadhana - Acad. Proc. Eng. Sci. **47** (2022)
100. P.R. Dewan, P.K. Kundu, On Titanium powder mixed electric discharge machining of Nimonic C-263, J. Inst. Eng. Ser. D (2022)
101. S. Singh, A. Pandey, Some studies into electrical discharge machining of Nimonic75 super alloy using rotary copper disk electrode, J. Mater. Eng. Perform. **22** (2013) 1290–1303
102. R.B.R. Chekuri, R. Kalluri, R. Siriyala, J.K. Palakollu, A study on die sinking EDM of Nimonic C-263 super alloy: an intelligent approach to predict the process parameters using ANN, Int. J. Eng. Technol. **7** (2018) 651–654

103. R.B.R. Chekuri, R. Kalluri, J.K. Palakollu, R. Siriyala, Modeling and optimization of machining high performance nickel based super alloy Nimonic C-263 using die sinking EDM, Int. J. Mech. Eng. Robot. Res. **8** (2019) 196–201
104. S. Sharma, U.K. Vates, A. Bansal, Optimization of machining characteristics for EDM of different nickel-based alloys by embodying of fuzzy, grey relational and Taguchi technique, World J. Eng. (2020)
105. A. Goswami, J. Kumar, Optimization in wire-cut EDM of Nimonic-80A using Taguchi's approach and utility concept, Eng. Sci. Technol. **17** (2014) 236–246
106. B. Singh, J.P. Misra, Empirical modeling of average cutting speed during WEDM of gas turbine alloy, MATEC Web Conf. **249** (2018) 1–5
107. A. Goyal, A. Pandey, P. Sharma, S.K. Sharma, Study on Ni-based super alloyusing cryogenic treated electrode by Taguchi methodology, Mater. Today Proc. **4** (2017) 2068-–2076
108. K.K. Jangra, V. Kumar, V. Kumar, An experimental and comparative study on rough and trim cutting operation in WEDM of hard to machine materials, Procedia Mater. Sci. **5** (2014) 1603–1612
109. A. Mandal, A.R. Dixit, S. Chattopadhyaya, A. Paramanik, Improvement of surface integrity of Nimonic C 263 super alloy produced by WEDM through various post-processing techniques, Int. J. Adv. Manuf. Technol. **93** (2017) 433–443
110. B. Singh, J.P. Misra, Empirical modelling of wear ratio during WEDM of Nimonic 263, Mater. Today Proc. **5** (2018) 23612–23618
111. V. Kumar, K.K. Jangra, V. Kumar, and N. Sharma, GA-based optimisation using RSM in WEDM of Nimonic-90: A nickel-based super alloy, Int. J. Ind. Syst. Eng. **28** (2018) 53–69
112. S. Singh Nain, R. Sai, P. Sihag, S. Vambol, V. Vambol, Use of machine learning algorithm for the better prediction of SR peculiarities of WEDM of Nimonic-90 superalloy, Arch. Mater. Sci. Eng. **95** (2019) 12–19
113. H. Singh, V. Kumar, J. Kapoor, Optimization of WEDM process parameters in machining Nimonic 75 alloy using brass wire, Multidiscip. Model. Mater. Struct. **16** (2020) 1189–1202
114. A. Goswami, J. Kumar, Surface topography and Kerf study of Nimonic 80A using Wire-cut EDM, Mater. Sci. Forum **808** (2015) 35–41
115. A. Goswami, J. Kumar, Investigation of surface integrity, material removal rate and wire wear ratio for WEDM of Nimonic 80A alloy using GRA and Taguchi method, Eng. Sci. Technol. **17** (2014) 173–184
116. A. Goswami, J. Kumar, Trim cut machining and surface integrity analysis of Nimonic 80A alloy using wire cut EDM, Eng. Sci. Technol. **20** (2017) 175–186
117. M.S. Rao, N. Venkaiah, Multi-response optimisation for MRR and Ra in WEDM process of nimonic-263 super alloy, Int. J. Mater. Prod. Technol. **56** (2018) 187–206
118. T. Sathish, BCCS approach for the parametric optimization in machining of Nimonic-263 alloy using RSM, Mater. Today Proc. **5** (2018) 14416–14422
119. T. Chaudhary, A.N. Siddiquee, A.K. Chanda, M.H. Abidi, A. Al-Ahmari, Multi-response optimization for Nimonic alloy miniature gear fabrication using wire electrical discharge machining, Adv. Mech. Eng. **12** (2020) 1–13
120. T. Chaudhary, A.N. Siddiquee, A.K. Chanda, S. Ahmad, I. A. Badruddin, Z.A. Khan, Multiple response optimization of dimensional accuracy of nimonic alloy miniature gear machined on wire Edm using entropy topsis and pareto Anova, Comput. Model. Eng. Sci. **126** (2021) 241–259
121. S. Ashok Sonawane, M.L. Kulkarni, Multi-quality response optimization of wire EDM for Ni-75 using PCA based utility theory, Mater. Today Proc. **5** (2018) 4584–4591
122. K. Mouralova et al., Precision machining of nimonic C 263 super alloy using WEDM, Coatings **10** (2020) 1–20
123. M. Singh, S. Singh, Multi-objective optimization of electro discharge machining of Nimonic 75 Using Taguchi-based Gray Relational analysis, J. Adv. Manuf. Syst. **20** (2021) 95–110
124. M. Singh, S. Singh, Multiple response optimization of ultrasonic assisted electric discharge Machining of Nimonic 75: A Taguchi-Grey relational analysis approach, Mater. Today Proc. **45** (2021) 4731–4736
125. A. Alhodaib, P. Shandilya, A.K. Rouniyar, H. Bisaria, Experimental investigation on silicon powder mixed-edm of nimonic-90 superalloy, Metals 11 (2021)
126. A. Goyal, A. Garimella, P. Saini, Optimization of surface roughness by design of experiment techniques during wire EDM machining, Mater. Today Proc. **47** (2021) 3195–3197
127. Senkathir, R. Manoj Samson, R. Nirmal, R. Ranjith, Parametric optimization of wire-EDM machining of Nimonic 80a using response surface methodology, IOP Conf. Ser. Mater. Sci. Eng. **1130** (2021)
128. R.K. Shastri, C.P. Mohanty, Sustainable electrical discharge machining of Nimonic C263 superalloy, Arab. J. Sci. Eng. 46 (2021) 7273–7293
129. V.K. Shukla, R. Kumar, B.K. Singh, Evaluation of machining performance and multi criteria optimization of novel metal-Nimonic 80A using EDM, SN Appl. Sci. **3** (2021) 1–10
130. B.P. Singh, J. Singh, J. Singh, M. Bhayana, D. Goyal, Experimental investigation of machining nimonic-80A alloy on wire EDM using response surface methodology, Met. Powder Rep. (2021) 1–9
131. R.V. Penmetsa, A.K. Ilanko, S. Rajesh, R.B.R. Chekuri, Experimental study and machining parameter optimization on powder-mixed EDM of Nimonic 901 using feed-forward backpropagation neural networks, Int. J. Adv. Manuf. Technol. (2022)
132. D. Sundaresan, L. Marappan, K. Thangavelu, V. Venkatraman, Machinability of Nimonic alloy 90 in μ-titanium carbide mixed electrical discharge machining, Arab. J. Sci. Eng. **47** (2022) 15223–15243
133. K. Satish, V.R. Srinivasan, C.P.S. Prakash, Optimization of machining parameters in machining Nimonic C-263 By WEDM process, J. Mines, Met. Fuels 70 (2022) 46
134. A.K. Singh, V. Sharma, Multi-objective optimization of grinding and vibration parameters of ultrasonic-assisted grinding with ultrasonically atomized novel green cutting fluid of Nimonic 80A, J. Brazilian Soc. Mech. Sci. Eng. **44** (2022) 1–20
135. J. Airao, N. Khanna, A. Roy, H. Hegab, Comprehensive experimental analysis and sustainability assessment of machining Nimonic 90 using ultrasonic-assisted turning facility, Int. J. Adv. Manuf. Technol. **109** (2020) 1447–1462

136. J. Airao, C.K. Nirala, L.N.L. de Lacalle, N. Khanna, Tool wear analysis during ultrasonic assisted turning of nimonic-90 under dry and wet conditions, Metals 11 (2021)
137. J. Airao, C.K. Nirala, Finite element modeling and experimental validation of tool wear in hot-ultrasonic-assisted turning of Nimonic 90, J. Vib. Eng. Technol. (2022) 0123456789
138. M. Singh, S. Singh, Comparative capabilities of conventional and ultrasonic-assisted-electrical discharge machining of Nimonic alloy 75, J. Mater. Eng. Perform. **31** (2022) 4611–4623
139. A.K. Singh, V. Sharma, A comparative appraisal of sustainable strategy in Ultrasonic Assisted Grinding of Nimonic 80A using novel green atomized cutting fluid, Sustain. Mater. Technol. **32** (2022) e00423
140. D.R. Unune, V.P. Singh, H.S. Mali, Experimental investigations of abrasive mixed electro discharge diamond grinding of Nimonic 80A, Mater. Manuf. Process. **31** (2016) 1718–1723
141. D.R. Unune, M. Marani Barzani, S.S. Mohite, H.S. Mali, Fuzzy logic-based model for predicting material removal rate and average surface roughness of machined Nimonic 80A using abrasive-mixed electro-discharge diamond surface grinding, Neural Comput. Appl. **29** (2018) 647–662
142. U.S. Yadav, V. Yadava, Modelling and optimisation of process parameters of electrical discharge diamond drilling of nimonic alloy – an aerospace material, Int. J. Ind. Syst. Eng. **29** (2018) 507–532
143. U.S. Yadav, V. Yadava, Experimental investigation on electrical discharge diamond drilling of nickel-based superalloy aerospace material, Proc. Inst. Mech. Eng. Part B J. Eng. Manuf. **231** (2017) 1160–1168
144. K. Mishra, B.R. Sarkar, B. Bhattacharyya, Influence of different featured tools on machining accuracy in electrochemical milling, Proc. Inst. Mech. Eng. Part B J. Eng. Manuf. (2019)
145. K. Mishra, S. Gupta, B. Bhattacharyya, Problematic areas in micro-electrochemical milling of HSTR alloys, Int. J. Adv. Manuf. Technol. **111** (2020) 1015–1036
146. C.S. Shamli, P. Hariharan, N. Yuvaraj, E. Rajkeerthi, Study and evaluation of process parameter on Nimonic 75 alloy by Electrochemical micromachining, IOP Conf. Ser. Mater. Sci. Eng. **923** (2020) 1–11
147. C. Ezhilarasan, A. Velayudham, M. Nagaraj, R. Anburaj, Analysis of Hole Taper, recast layer and heat affected zone in pulsed O2 and N2 laser drilling of difficult-to-cut alloy Nimonic C-263, 3rd Int. Conf. Mater. Manuf. Eng. **390** (2018) 1–10
148. T. Sibalija, S. Petronic, D. Milovanovic, Experimental optimization of nimonic 263 laser cutting using a particle swarm approach, Metals (Basel) 9 (2019)
149. A. Bagchi, M. Srivastava, R. Tripathi, S. Chattopadhyaya, Effect of different parameters on surface roughness and material removal rate in abrasive water jet cutting of Nimonic C263, Mater. Today Proc. **27** (2019) 2239–2242
150. S. Madhavarao, R.V. Penmetsa, C. Rama Bhadri Raju, H.T. R. Gottumukkala, Optimization of process variables in abrasive water jet machining of Nimonic C-263 super alloy using Taguchi method, in Proceedings of Fourth International Conference on Inventive Material Science Applications, Advances in Sustainability Science and Technology (2022), pp. 167–177
151. M. Nagaraj, C. Ezilarasan, A. John Persin Kumar, A. Velayudham, A review of machining characteristics in mechanical drilling of super alloys, Int. J. Mech. Prod. Eng. Res. Dev. **8** (2018) 579–588
152. A.K. Singh, A. Kumar, V. Sharma, P. Kala, Sustainable techniques in grinding: State of the art review, J. Clean. Prod. **269** (2020) 121876

Cite this article as: Ganesha Prasad, Raghavendra Kamath C, Vijay G.S. A review on conventional and nonconventional machining of Nickel-based Nimonic superalloy, Manufacturing Rev. **10**, 10 (2023)